https://doi.org/10.5194/egusphere-2026-932
Preprint. Discussion started: 10 June 2026

Multiscale atmospheric modeling suggests ammonia is necessary but not sufficient to explain new particle formation in the Colorado boundary layer

Han Ding [1,2], Pratapaditya Ghosh [3,2,*], Xu-Cheng He [2,4,5], R Lee Mauldin III [5,6], David O'Neal [7,†], John Ortega [8], James N Smith [9], and Hamish Gordon [10,2]

[1]Department of Mechanical Engineering, Carnegie Mellon University, Pittsburgh, Pennsylvania, United States
[2]Center for Atmospheric Particle Studies, Carnegie Mellon University, Pittsburgh, Pennsylvania, United States
[3]Department of Civil and Environmental Engineering, Carnegie Mellon University, Pittsburgh, Pennsylvania, United States
[4]Yusuf Hamied Department of Chemistry, University of Cambridge, Cambridge, CB2 1EW, United Kingdom
[5]Institute for Atmospheric and Earth System/Physics, Faculty of Science, University of Helsinki, Helsinki, Finland
[6]Department of Atmospheric and Oceanic Sciences, University of Colorado, Boulder, Colorado, United States
[7]Pittsburgh Supercomputing Center, Pittsburgh, Pennsylvania, United States
[8]Institute of Arctic and Alpine Research, Stable Isotope Lab, University of Colorado, Boulder, Colorado, United States
[9]Department of Chemistry, University of California, Irvine, California, United States
[10]Department of Chemical Engineering, Carnegie Mellon University, Pittsburgh, Pennsylvania, United States
[*]Now at Lawrence Livermore National Laboratory
[†]Deceased

Correspondence: Hamish Gordon (gordon@cmu.edu) and Han Ding (handing@andrew.cmu.edu)

Abstract. New particle formation (NPF) is an important source of cloud condensation nuclei (CCN) in the atmosphere, and CCN affect Earth's radiative balance via aerosol-cloud interactions. Numerous chemical species are involved, but most climate models still represent NPF only from sulfuric acid and water. However, the roles of ammonia and ions in NPF alongside sulfuric acid are also well-quantified compared to other species. Here, we tested a parameterization of ternary NPF from sulfuric acid, ammonia, ions and water in the UK Met Office Unified Model using surface and aircraft measurements from the 2014 FRAPPÉ and DISCOVER-AQ field campaigns. We used a nested convection-permitting regional model setup with a grid spacing of 3 km, which allowed us to represent the inhomogeneous sources of emissions in the area. The aircraft simultaneously measured sulfuric acid and ammonia vapor concentrations and aerosol size distributions, so we can test whether NPF from these species can explain observed aerosol number concentration. We also compared particle number concentrations in a lower resolution global simulation to surface observations. In our model, errors in the NPF mechanism are compensated by errors in simulated concentrations of gas-phase precursors. We devised a method to disentangle these errors, but only qualitative results were obtained with the datasets we used. While our results suggest ammonia and sulfuric acid are likely important to NPF in Colorado and elsewhere, other species must also make important contributions. Overall, however, the ternary NPF mechanism gives a substantial improvement on the Unified Model's existing representation of aerosol number concentrations.

https://doi.org/10.5194/egusphere-2026-932
Preprint. Discussion started: 10 June 2026

1 Introduction

Aerosol-cloud interactions are primary causes of uncertainty in understanding past and future changes in Earth's radiative balance (Forster et al., 2021; Bellouin et al., 2020; Boucher et al., 2014). These interactions depend on cloud droplet number concentrations, and thus in turn on aerosol number concentrations, which are not accurately simulated in many atmospheric and climate models (Williamson et al., 2019). Approximately half of atmospheric cloud condensation nuclei (CCN) at the altitude of low clouds are thought to originate from new particle formation (NPF) (Merikanto et al., 2009; Wang and Penner, 2009; Yu and Luo, 2009; Gordon et al., 2017) via gas-to-particle conversion. Formation rates of the smallest aerosol particles that climate models represent vary nonlinearly with precursor gas concentrations, temperature, relative humidity, and pre-existing aerosol concentrations (Pierce and Adams, 2007; Westervelt et al., 2013; Stolzenburg et al., 2023). The large biases in climate model simulations of aerosol number concentrations are in part because accurate simulation of all of these variables is challenging, and the parameterizations of NPF rates that use these inputs are also uncertain. The non-linear dependence of NPF rates on environmental conditions also causes NPF to be episodic: the rates, and thus the importance of the NPF process, vary by many orders of magnitude with location and time. Therefore, to improve the representation of NPF in climate models, detailed modeling studies of particle formation events in specific regions over short time periods are potentially useful first steps.

Most climate models that participated in version 6 of the Coupled Model Intercomparison Project (CMIP6) only represented the dependence of NPF on sulfuric acid and water (McMurry and Friedlander, 1979; Clarke, 1993; Brock et al., 1995; Vehkamäki et al., 2002; Semeniuk and Dastoor, 2018). Many other compounds, and also ions from cosmic rays or radon (Mohnen, 1977), can stabilize sulfuric acid clusters, and some compounds can also form aerosols without sulfuric acid. As the spatial and temporal variability in the concentrations of these compounds often differs substantially from that of sulfuric acid, representing the contribution of these compounds to NPF in simulations can improve how simulated aerosol number concentrations vary over space or time.

Besides sulfuric acid and water, the roles of ammonia and ions in NPF are perhaps the best understood. Early studies inferred that ammonia was important to NPF (e.g. Scott and Cattell, 1979), and field observations subsequently demonstrated NPF rates correlated well with ammonia concentrations (Weber et al., 1996). Controlled experiments in laboratories (Ball et al., 1999; Kirkby et al., 2011) have yielded parameterizations of NPF associated with ammonia and ions (Chen et al., 2012; Dunne et al., 2016). NH_3 is also frequently measured in nucleating clusters during field campaigns (Schobesberger et al., 2013; Yan et al., 2021), especially in urban areas with high levels of air pollution or agricultural activities.

Several versions of chemical transport and Earth system models are beginning to include parameterizations that represent the contributions of ammonia and ions to NPF, sometimes alongside other species (Baranizadeh et al., 2016; Zhao et al., 2020; Ehrhart et al., 2018; Nair et al., 2023; Shao et al., 2024; Zhao et al., 2024; Patoulias et al., 2025; Mao et al., 2025). However, parameterizations of this type have not yet been tested in the UK Met Office Unified Model except in remote marine conditions where ammonia concentrations are usually low or negligible (He et al., 2025). The Unified Model, like an increasing number of other Earth System models, can be configured to represent both global climate, as the UK Earth System Model (UKESM1, Sellar et al. (2019)) or to represent regional weather and air quality with grid spacing around or below a kilo-

https://doi.org/10.5194/egusphere-2026-932
Preprint. Discussion started: 10 June 2026

meter (convection-permitting or cloud-resolving) resolution. The latter allows detailed studies of atmospheric processes like aerosol-cloud interactions and NPF (Gordon et al., 2023; Wang et al., 2023) and more precise model evaluations against point observations (especially in areas with heterogeneous terrain or emissions) with smaller representativeness uncertainties (Schutgens et al., 2016).

Here we included a parameterization of NPF that represents the participation of ammonia and ions in the Unified Model. We evaluated the model performance in a high resolution configuration with 3 km grid spacing over Colorado during case studies of NPF events observed by aircraft during the Deriving Information on Surface Conditions from COlumn and VERtically Resolved Observations Relevant to Air Quality (DISCOVER-AQ) and Front Range Air Pollution and Photochemistry Experiment (FRAPPÉ) field campaigns (Flocke et al., 2020). We examined the extent to which the agreement of simulated aerosol number concentration with observations validates the model's representation of NPF. Finally, we briefly explored the implications of the updated NPF mechanism for global aerosol number concentrations, focusing on surface observations.

2 Method

2.1 Model setup

We used the Nested Unified Model with Aerosols and Chemistry (NUMAC) setup (Gordon et al., 2023) of the Met Office Unified Model (UM) version 11.9 to simulate NPF events in Colorado. In NUMAC, a convection-permitting regional model with prognostic double-moment aerosol microphysics is nested inside a global model. The global model provides lateral boundary conditions to the regional model, and there is no feedback from the regional model to the global model (one-way nesting). The global model has the same grid as the UKESM1 model ('N96' horizontal resolution of approximately $135\,\mathrm{km} \times 187.5\,\mathrm{km}$, and 85 vertical levels up to 85 km, of which 10 are within 1 km of the surface). Both regional and global model are run in an atmosphere-only configuration with fixed sea surface temperatures but an interactive land surface. While some parameterizations differ between the regional and global model as described below, most of the code is the same for both.

Here, the regional model has 3 km resolution and is centered at $(40°\mathrm{N}, 105°\mathrm{W})$ with 300 grid cells in each horizontal direction; the domain is shown in Figure 1. Both global and regional models were initialized to an operational numerical weather prediction analysis produced using the UM on 16 July 2014. The global model configuration used the Global Atmosphere version 7.2, which is almost identical to the GA7.1 setup documented by Walters et al. (2019), while the regional model used the Regional Atmosphere and Land configuration version 2 for the mid-latitudes (RAL2-M) (Bush et al., 2023). The simulations were run from 16 July to 9 August 2014. Aerosol, chemical and meteorological fields were diagnosed from the global and regional models every three hours.

Aerosols and chemistry were initialized from a prior global UM simulation using a prototype version of the UKESM1 atmosphere model similar to that described by Ranjithkumar et al. (2021), in which meteorological fields were nudged to reanalysis. The regional and global models were then run in a forecasting setup (Gordon et al., 2023; Giuffrida et al., 2025), in which both models' meteorological fields were reinitialized to operational UM analysis every 48 hours from 16 July until 9

https://doi.org/10.5194/egusphere-2026-932
Preprint. Discussion started: 10 June 2026

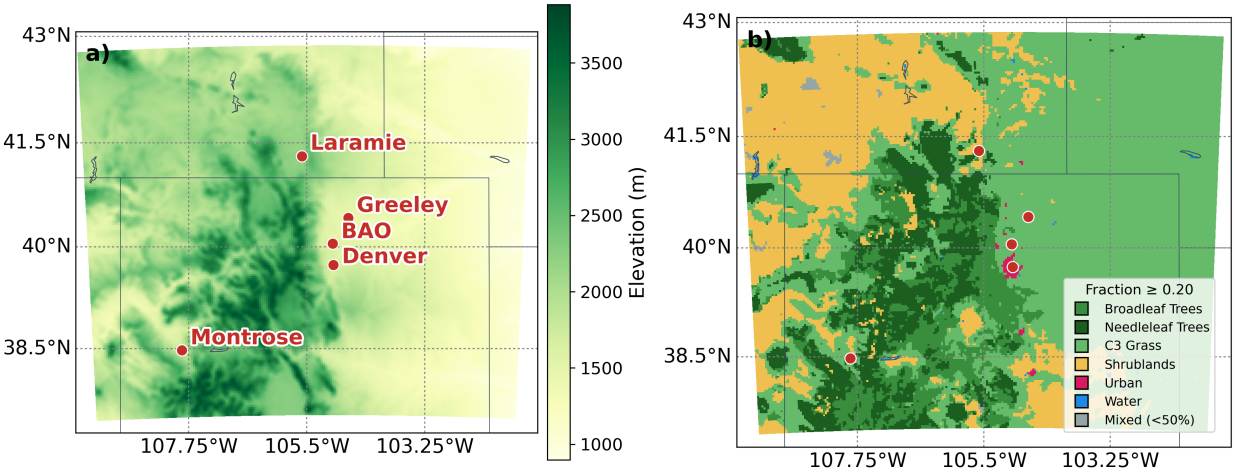

Figure 1. The simulation domain over the Colorado region as represented in our regional model, showing a) the topography as altitudes above sea level and selected locations and b) selected land surface types from the land surface model. Subfigure a) shows the location of the Boulder Atmospheric Observatory (BAO) tower as well as urban centers, as we use measurements from the tower. Usually only one land surface type occupies more than 20% of a grid cell, in which case it is shown. Globally, grasses are categorized by the simplest configurations of the JULES model as either C_3 (temperate) or C_4 (tropical); temperate grasses are prevalent in this region. Solid grey lines correspond to boundaries of US states.

August 2014. Each forecast within these intervals was run for 60 hours and the first 12 hours of each forecast was discarded as a spin-up. Aerosol and chemical fields are carried over from the previous forecast.

Table 1 summarizes key features of the model with some relevant references. Overall, the NUMAC model setup we used is very similar to the original version described by Gordon et al. (2023), except that the UM version was updated to 11.9 from 11.6 and the configuration from RAL1 to RAL2 (both of these involve only relatively minor changes relevant to this setup), the aerosol and chemical emissions were adapted as described below, and nitrate and ammonium aerosol were represented. For completeness, a brief description of the model is provided in the following sections 2.2 and 2.3.

To evaluate global aerosol number concentration with surface measurements, we used a 1-year atmosphere-only simulation of 2015 started in September 2014 that was nudged to ERA5 horizontal winds above the boundary layer following (Telford et al., 2008). To simulate a year, it is more convenient to use a derivative of the UKESM1 atmosphere setup than a NUMAC setup, which is intended for shorter simulations, and nudging rather than forecasting (as the forecast intialization files required every few days in a forecasting setup for 2015 are each around 30GB in size). Therefore, the UM version used was 13.0 and the scientific configuration was GA7.1. Otherwise the setup is identical to the NUMAC driving global model (for example, the same

https://doi.org/10.5194/egusphere-2026-932
Preprint. Discussion started: 10 June 2026

Table 1. Summary of key features of our Unified Model setup over the Colorado region.

Configurations	Global model	Regional model
Horizontal resolution	N96 (144 × 192 boxes)	0.027° × 0.027°
	(∼135 km × 187.5 km)	(∼3 km × 3 km)
Vertical resolution	85 levels up to 85 km	70 layers up to 40 km
	(10 levels in first km)	(15 levels in first km)
Dynamical timestep	20 min	60 s
Reinitialization	Every 48 hours	Every 48 hours
Large-scale clouds	PC2 (Wilson et al., 2008)	Smith (1990)
Cloud microphysics	Wilson and Ballard (1999)	CASIM (Field et al., 2023)
Chemistry	UKCA/StratTrop	UKCA/StratTrop
Aerosols	GLOMAP (5-mode, 7-species)	GLOMAP (5-mode, 7-species)
	(CLASSIC dust)	(CLASSIC dust)
Emissions	CMIP6 2014	EDGAR 2014 where available
	(N96 resolution)	(0.01° resolution)

grid resolution, the same CMIP6 emissions, updated where appropriate as described below, and physical parameterizations are used). Nudged and forecasting simulations were shown to transport aerosol very similarly in a different case study by Giuffrida et al. (2025).

2.2 Meteorological model

The UM uses a semi-Lagrangian, semi-implicit, nonhydrostatic dynamical core (Wood et al., 2014; Thuburn, 2016). No parameterized convection is employed in the regional model. The land surface is represented using the Joint UK Land Environment Simulator (JULES) (Best et al., 2011; Clark et al., 2011). The representation of boundary layer turbulence is described by Lock et al. (2000) and radiation by Manners et al. (2017). In the regional model, precipitation is represented with the scheme of Field et al. (2023) and sub-grid cloud fraction with the scheme of Smith (1990). In the global model, precipitation is represented according to Wilson and Ballard (1999) and sub-grid cloud fraction according to Wilson et al. (2008). These combinations of schemes are consistent with other recent multiscale UM modeling studies with prognostic aerosols (Gordon et al., 2020, 2023; Ghosh et al., 2025).

https://doi.org/10.5194/egusphere-2026-932
Preprint. Discussion started: 10 June 2026

2.3 Chemistry and aerosols

Chemistry and aerosols in the UM are simulated using the UK Chemistry and Aerosols (UKCA) submodel. We used the StratTrop chemistry scheme (Archibald et al., 2020) with a chemistry timestep of 1 hour in the global model and 2 minutes in the regional model. The key secondary nucleation precursor, gas-phase sulfuric acid (H_2SO_4), is formed only by the oxidation of sulfur dioxide (SO_2) with OH radicals. Within UKCA, aerosols are represented using the Global Model of Aerosol Processes (GLOMAP-mode) scheme (Mann et al., 2010; Bellouin et al., 2013; Mulcahy et al., 2020). GLOMAP represents the aerosol particle size distribution using five log-normal modes. The scheme is double-moment in that the number and mass of the particles are prognostic, while the geometric standard deviations of each mode are constants.

Aerosol composition is represented to the extent that the model tracks sulfate (SO_4^{2-}), ammonium (NH_4^+), nitrate, black carbon (BC), organic carbon (OC) and two sea spray (SS) species. All species are assumed to be internally mixed within the modes, while dust is simulated separately as in UKESM (Mulcahy et al., 2020). The scheme representing nitrate and ammonium aerosol with two sea spray components is described by Jones et al. (2021) and was recently tested in high-resolution regional simulations over Paris by Ghosh et al. (2025). Gaseous ammonia (NH_3) and nitric acid (HNO_3) are assumed to reach equilibrium with the particle phase instantaneously within each chemistry time step, although an uptake coefficient limits the rate at which nitric acid partitions to the aerosol phase. We set this uptake coefficient to 0.001, the 'slow' value from Jones et al. (2021), in this study, as this produces higher ammonia concentrations in better agreement with observations.

By default, the model uses emissions from the Coupled Model Intercomparison Project version 6 (CMIP6) inventories for 2014, which are available monthly on the N96 grid of the global model. In the regional model, where possible we replaced these with emissions from the Emissions Database for Atmospheric Research (EDGAR) Hemispheric Transport of Air Pollution (HTAP) version 3 for 2014, which are available at $0.1^\circ \times 0.1^\circ$ and monthly resolution (Huang et al., 2017). The EDGAR species comprise anthropogenic primary black and organic carbon aerosol emissions, and anthropogenic SO_2, NH_3, NO_x, non-methane VOC, and CO emissions. As in the UM simulations submitted to CMIP6 (Mulcahy et al., 2020), all species are emitted at the surface except primary BC and OC emissions from forest burning and SO_2 from volcanoes. Following Denier van der Gon et al. (2011), we applied diurnal cycles to BC, OC, and NO_x emissions from fossil fuel burning according to the Selected Nomenclature for Sources of Air Pollution (SNAP) cycle SNAP7 for road transport, and to NH_3 emissions according to the SNAP10 cycle in the regional model. The diurnal cycles are shown in Supplement Figure S1. In the global model, we updated primary BC, OC and SO_2 emissions to match the April 2025 release of Community Earth atmospheric Data System (CEDS, v_2025_04_18) anthropogenic emission inventories, in view of the significant improvements to the CEDS inventories since CMIP6 for these species.

2.4 NPF parameterizations

Particle formation in the UM with UKCA is by default represented using the Vehkamäki et al. (2002) parameterization (referred to as V2002) for the formation of particles from sulfuric acid and water based on classical nucleation theory combined with *ab initio* calculations and experimental data. Ranjithkumar et al. (2021) additionally tested a representation of particle

https://doi.org/10.5194/egusphere-2026-932
Preprint. Discussion started: 10 June 2026

formation of sulfuric acid and organic molecules (Metzger et al., 2010), restricted to the planetary boundary layer. While this parameterization is less well-grounded in theory than that of V2002, it was found to improve agreement of aerosol number concentrations with observations at high latitudes. Previous studies with GLOMAP have also tested more comprehensive representations of NPF, but only using the TOMCAT chemical transport host model at 2.8° spatial resolution, not the UM (Dunne et al., 2016; Gordon et al., 2017).

Here we represented the participation of ammonia and ions in NPF in the UM using the parameterization of Dunne et al. (2016), referred to as D2016. While it is expected from previous work (Gordon et al., 2017) that this will not be sufficient to explain NPF rates in the boundary layer, it is an important first step towards a more comprehensive parameterization. We delay representing NPF from organic molecules to future studies, in anticipation of updated results from the Cosmics Leaving OUtdoor Droplets (CLOUD) experiment relative to the current published parameterizations of Riccobono et al. (2014) and Lehtipalo et al. (2018) that will, for example, quantify the temperature dependence of the contributions to NPF from these organic molecules.

While ammonia gas concentrations are already represented in the UM (Jones et al., 2021), ion concentrations are not. To simplify the representation of ions in the UM, we used a climatology of ion production rates from cosmic rays and radon generated from the TOMCAT simulations presented by Gordon et al. (2017). The radon ion production rates in this climatology are monthly means originating from the lookup tables of Zhang et al. (2011) for the average of 1999-2001 while the cosmic ray source was represented in TOMCAT based on the methods of Usoskin et al. (2010) as described by Dunne et al. (2016) (their Supplement, Section 13) and is for the year 2008. We then determined ion concentrations by assuming a steady state between production and the ion removal processes, namely ion-ion recombination (with coefficient α from Brasseur and Chatel (1983)) and the ion condensation sink (CS_{ion}) onto existing particles, which replaces the wall loss rate in the description of this process by Dunne et al. (2016) (their Supplement, Section 8). The CS_{ion} is calculated based on Hoppel and Frick (1986).

With the ion concentrations in place, we followed previous work with GLOMAP in using the representation of binary and ternary ion-induced NPF of D2016. This parameterization predicts NPF rates at 1.7 nm diameter and was determined directly by fitting data from the CLOUD chamber. The parameters are given at full precision by Gordon et al. (2017). Future efforts should explore approaches that reinforce these parameterizations with theoretical calculations (Määttänen et al., 2018; Yu et al., 2018).

The overall nucleation rate is given by the sum of the following individual processes:

$$J_{1.7} = J_b + J_t \tag{1}$$

$$J_b = J_{b,i} + J_{b,n} = k_{b,n}(T)[H_2SO_4]^{p_{b,n}} + k_{b,i}n^-[H_2SO_4]^{p_{b,i}} \tag{2}$$

$$J_t = J_{t,i} + J_{t,n} = k_{t,n}(T)f_n([NH_3],[H_2SO_4])[H_2SO_4]^{p_{t,n}} + k_{t,i}n^- f_i([NH_3],[H_2SO_4])[H_2SO_4]^{p_{t,i}} \tag{3}$$

where $J_{b,n}$ is the binary neutral nucleation rate, $J_{b,i}$ is the binary ion-induced rate, $J_{t,n}$ is the ternary neutral rate and $J_{t,i}$ is the ternary ion-induced rate. n^- represents the steady-state concentration of small negative ions. The functions $k(T)$ and f and the power parameters p are detailed in D2016 and Gordon et al. (2017). Approximately, the binary neutral rate is proportional to the fourth power of sulfuric acid while the other component rates are proportional to the third power. Ternary rates are

https://doi.org/10.5194/egusphere-2026-932
Preprint. Discussion started: 10 June 2026

approximately linear in ammonia concentration and ion-induced rates are exactly linear in ion concentration. All rates increase strongly as temperature is reduced. The parameterization requires H_2SO_4 and NH_3 in units of 10^6 cm^{-3}.

The 1.7 nm diameter formation rate must be converted to a 3 nm diameter formation rate before the newly formed particles can be added to the nucleation mode in GLOMAP. As in the existing code used with the V2002 parameterization, this is accomplished via the parameterization of Kerminen and Kulmala (2002):

$$J_3 = J_{1.7} \cdot \exp\left(0.23 \cdot \left(\frac{1.0}{3.0} - \frac{1.0}{1.7}\right) \cdot \frac{CS}{\mathrm{GR_{tot}}}\right) \tag{4}$$

$$\mathrm{GR_{tot}} = (2.68 \cdot 2.35^{-1.27} + 0.81) \cdot \left(\frac{[H_2SO_4]}{10^7}\right) \tag{5}$$

where J_3 is the nucleation rate for 3 nm particles, CS represents the condensation sink of the particles, which is calculated following Equations (50) to (56) in Section 2.2.7 of Mann et al. (2010). The total growth rate of the particles, indicated as $\mathrm{GR_{tot}}$, is assumed to depend solely on the concentration of sulfuric acid at these small sizes and is parameterized approximately following Equation 16 of Stolzenburg et al. (2020), where 2.35 nm is the central value of the diameter range over which the particles are growing. The sulfuric acid concentration in Equation 5 is in the more usual units of cm^{-3}. The effects of organic molecules, ammonia, or relative humidity on this growth rate are potentially important (e.g. Tröstl et al., 2016) and would be valuable to include in future simulations.

Relative humidity (RH) has an important influence on nucleation rates, and at least for the ternary system it is not well constrained by laboratory measurements. In D2016, a correction factor for the effect of RH on the NPF rates was given as

$$K_{RH} = 1 + c_1(RH - 0.38) + c_2(RH - 0.38)^3(T - 208)^2 \tag{6}$$

$$\text{If } K_{RH} < 0, \text{then } K_{RH} = 0 \tag{7}$$

with $c_1 = 1.51$ and $c_2 = 0.045449$ and where T represents temperature in Kelvin. The temperature dependence accounts for increased water vapor at higher temperatures, which can enhance nucleation rates. The lower limit is imposed to ensure the correction factor remains non-negative. We applied this correction factor here, as it is most likely better than not doing so, but caution that it remains very uncertain.

2.5 Field measurements in Colorado

The simultaneous DISCOVER-AQ and FRAPPÉ field campaigns over the Denver region and the Colorado Front Range were motivated by the need to understand atmospheric trace gas and aerosol concentrations in a region with complex emissions and topography (Flocke et al., 2020). The complex cocktail of anthropogenic emissions includes traffic emissions and volatile chemical products primarily from the Denver metropolitan area, emissions from oil and gas extraction in the Denver-Juleburg basin, coal power plants such as the 500 MW Pawnee station east of Denver, and intensive agriculture especially in the Greeley area (Weld County). Biogenic emissions from forests, mainly west of Denver, also likely impact secondary organic aerosol. Mesoscale circulations related to the Front Range topography such as the Denver Cyclone can lead to accumulation of pollutants and poor air quality (Vu et al., 2016). While NPF and growth might be expected to be muted by the high levels of primary

https://doi.org/10.5194/egusphere-2026-932
Preprint. Discussion started: 10 June 2026

particulate pollution, NPF still occurred fairly frequently during the study due to the high concentrations of sulfuric acid from coal power generation, ammonia from agriculture, and likely also other low-volatility molecules or known NPF precursors emitted from oil and gas extraction, trees, and other sources. For example, on the eastern slopes of the Rocky Mountains, which experience frequent daytime upslope flows from the Denver area, Boy et al. (2008) observed 10 clear event days and 14 undefined days out of 32 days from 25 June to 26 July 2006. According to the classification of Dal Maso et al. (2005), a day contains an NPF event if a distinctly new mode of particles appears in the size distribution, starting in the nucleation mode size range, and it persists and grows over several hours. Undefined days contain evidence of NPF but not a clear event with growth.

While the high complexity of the chemistry and topography makes a simulation of this region challenging, the campaigns remain attractive for model evaluation due to the comprehensive instrumentation used. A complete list of measurements made during the campaigns is presented by Flocke et al. (2020). Most relevant here, the NCAR C-130 aircraft (the key platform for the FRAPPÉ campaign) was equipped with simultaneous online measurements of sulfuric acid at 30s time resolution from a HOx-ROx Chemical Ionization Mass Spectrometer (CIMS), SO_2 from another CIMS, ammonia from a dual quantum-cascade laser mid-infrared absorption spectrometer, total aerosol number concentration and the aerosol size distribution down to around 10 nm particle mobility diameter from a Scanning Mobility Particle Sizer (SMPS), and other relevant measurements of meteorology and larger aerosols including their composition. The NASA P3-B (the key platform for the DISCOVER-AQ campaign) similarly had a full aerosol size distribution and an online measurement of ammonia, and aerosol size distributions were also measured at several locations on the ground. Simultaneous measurements of all of these variables are rare. A summary of the datasets we use here is given in Table 2.

Table 2. Summary of instrumentation used on the two aircraft and at the Boulder Atmospheric Observatory (BAO) tower. Only the most relevant instruments for our analysis are listed; complete lists are provided by Flocke et al. (2020).

Variables	**Campaign**		
	FRAPPÉ (C-130)	**DISCOVER-AQ (P-3B)**	**BAO tower**
Aerosol Size distribution	✓	✓	✓
Aerosol Number concentration	✓	✓	×
NH_3	✓	✓	✓
H_2SO_4, SO_2	✓	only SO_2	only SO_2
Aerosol Composition	✓	×	×

On the NASA P3-B, the number concentration of nucleation-mode particles can be determined by taking the difference of the two TSI condensation particle counters with cut-off sizes of 3 nm and 10 nm. These data, like the SMPS data and the TSI Laser Aerosol Spectrometer (LAS) Model 3340 that were used to measure larger particles on the P3-B, are available from the NASA archives at ambient temperature and pressure.

https://doi.org/10.5194/egusphere-2026-932
Preprint. Discussion started: 10 June 2026

On the C-130, the aerosol number concentrations were measured using a butanol TSI 3760 CPC with a 50% cut-off diameter of 11 nm. The size distributions were determined using an SMPS including a nano-DMA (TSI model 3085) with the lowest size bin at around 9 nm and highest at 100 nm, and a Passive Cavity Aerosol Spectrometer Probe (PCASP) for particles greater than 100 nm in diameter. The CPC and PCASP recorded data at ambient temperature and pressure (Cooper, 2022). The SMPS had a scanning time of 60s, leading to a time resolution of measurements of just over 60s, while the other aerosol instruments measure with 1s time resolution. These instruments were also used in the Airborne Research Instrumentation Testing Opportunity (ARISTO) campaign in 2016. Details of their operation are discussed in the context of ARISTO by Ortega et al. (2019). The SMPS measured particle concentrations at a temperature and pressure similar to that in the aircraft cabin; we approximated these as 293 K and cabin pressure and converted the measurements to ambient conditions, then verified using the temperature and pressure measurements from the instrument from two flights that our approximation led to uncertainties below 20%. During FRAPPÉ, the total aerosol concentration measured by the CPC substantially exceeded the sum of the concentrations measured by the SMPS and the PCASP, perhaps because the lower cut-off of the DMA is sharper (as a function of particle size) than that of the CPC. To infer concentrations of particles that are approximately 'nucleation-mode' from the C-130, which we speculate would have diameters in the range between 8 nm and 12 nm, we obtained two estimates that differ quite substantially, sometimes by a factor 5-10. The high estimate comes from the difference between the concentration recorded by the CPC and the sum of the particle concentrations in the SMPS and PCASP. The low estimate comes from the total number of counts in the lowest two SMPS size bins, which have a combined width of 4 nm and central value of approximately 10 nm. The uncertainties in both of these estimates are likely large, and in view of this we made no attempt to make our calculation more precise by (for example) accounting for differences between aerodynamic and mobility diameter. Nonetheless, there is a good chance that these estimates bound the true values.

Several prior studies have examined the DISCOVER-AQ/FRAPPÉ datasets and the ability of models to represent atmospheric composition during the campaigns. Those most pertinent to this study concern transport, aerosols and ammonia. Pfister et al. (2017) examined the ability of the WRF model at 3 km grid resolution to represent transport in the complex meteorological environment, and found the model performed reasonably well, modeling the boundary layer height and important upslope winds well most of the time. These good results suggest our choice of 3 km resolution for the UM regional model is also reasonable. Valerino et al. (2017) examined aerosol sources and highlighted the importance of dust from long-range transport during the period of the field campaign we analyze here. Bahreini et al. (2018) estimated the contribution of oil and gas emissions and biogenic secondary organic aerosol (SOA) to total organic aerosol and found biogenic SOA to be important, suggesting also a potential role for biogenic organic species in NPF in concert with sulfuric acid and ammonia (e.g. Lehtipalo et al., 2018). WRF-chem simulations represented organic aerosol mass relatively poorly unless tuned, with underestimates of a factor two at best. We can expect similar poor performance from the relatively crude, and untuned, representation of organic aerosol in the UM. Also, Battye et al. (2016) evaluated simulations of ammonia concentrations in the NOAA National Air Quality Forecast Capability (NAQFC) with National Emission Inventory (NEI) emissions from 2005. Aircraft measurements from DISCOVER-AQ were used together with ground measurements. The simulated ammonia concentrations were on average a factor 2.7 lower than the aircraft observations, again leading us to expect similar behavior in the UM. Further analysis of

https://doi.org/10.5194/egusphere-2026-932
Preprint. Discussion started: 10 June 2026

ground-based measurements during the campaigns highlight the important variability of ammonia emissions over the diurnal cycle (Eilerman et al., 2016) and within the near-surface layer (Tevlin et al., 2017). If no diurnal cycle in methane concentrations (which were used for calibration) is assumed, ammonia emissions were inferred to be a factor four higher during the day than at night, and daytime concentrations vary over around a factor two within 100 m of the surface.

2.6 Evaluation of global annual mean aerosol number concentration

As we aim to lay foundations to update the V2002 NPF parameterization in the UM to a more sophisticated mechanism starting from the ternary NPF scheme we test here, it is worthwhile to examine how the ternary NPF scheme by itself affects global surface aerosol number concentrations. The EBAS (European Monitoring and Evaluation Programme) database, maintained by the Norwegian Institute for Air Research (NILU), is a comprehensive repository of atmospheric data including number concentrations (Tørseth et al., 2012). The sites were categorized into three main regions: global remote regions, North American sites, and European sites, to cover a broad range of atmospheric conditions, from pristine environments like the South Pole to more urbanized and industrialized areas in Europe and North America. Measurements were made as part of the European Monitoring and Evaluation Programme (EMEP), Global Atmosphere Watch – World Data Centre for Aerosols (GAW-WDCA) and Aerosol, Clouds and Trace Gases Research Infrastructure (ACTRIS) programs. Here we follow Kohl et al. (2023) in evaluating annual mean number concentrations in 2015. We compared three nudged global UM simulations of 2015: a simulation with NPF represented according to V2002, a simulation with only binary NPF of sulfuric acid and water represented according to D2016, and a simulation with the full parameterization of D2016 including the role of ammonia.

3 Results

3.1 Classification of New Particle Formation (NPF) Events from DISCOVER-AQ and FRAPPÉ 2014 Campaign Measurements

During the period of overlap of the DISCOVER-AQ and FRAPPÉ 2014 campaigns, 27 July to 8 August, we analyzed the P3-B and C-130 aircraft data sets together with some contextual datasets from ground measurements. A summary of the P3-B flight days is given in Table 3. We performed a basic evaluation of the model across all of these days in the next section, and used the table to select two NPF days for more detailed analysis.

In Table 3, the Wind Direction (WD) and key precursors of NPF, SO_2 and NH_3 are averages over the duration of the corresponding P3-B flight of ground-level measurements at the BAO tower (40.03°N, -105.00°W). The WD represents the average value for each day within the available dataset's time period. The condensation sink CS is calculated consistently with code in our model following Mann et al. (2010). The P3-B observed significant numbers of nucleation-mode aerosols on all days. Supplementary Figures S2-S4 show observed size distributions and simulated and observed total aerosol number concentrations during all nine P3-B flights analysed, while the NPF event that is a focus of this study is also shown in Figure 3. Here, we aim to investigate widespread NPF events. Short-lived spikes in total aerosol number concentration likely originate

https://doi.org/10.5194/egusphere-2026-932
Preprint. Discussion started: 10 June 2026

Table 3. Classification of NPF and non-NPF days based on measurements from the DISCOVER-AQ 2014 campaign with the NASA P3-B aircraft and at the Boulder Atmospheric Observatory (BAO) tower. Aircraft measurements are presented as averages over all altitudes, and altitudes below 2500 m above sea level. Measurements from the tower are averages over the duration of the P3-B flight on the day.

Date	Classification	P3-B aircraft				BAO tower			
		N_{3-10} (# cc^{-3})	N_{3-10} <2500m (# cc^{-3})	CS (s^{-1})	CS <2500m (s^{-1})	WD (°)	WD (dir)	SO_2 (ppb)	NH_3 (ppb)
07/27	NPF	725	1095	1.04×10^{-3}	1.74×10^{-3}	149.5	SSE	1.03	1.96
07/28	Undefined	1296	1934	9.06×10^{-3}	9.44×10^{-3}	168.9	S	0.95	6.70
07/29	Non-NPF	1205	1646	1.54×10^{-2}	1.56×10^{-2}	145.0	SE	0.87	4.31
07/31	NPF	1938	3052	6.11×10^{-3}	7.00×10^{-3}	194.2	SSW	1.18	1.30
08/02	Undefined	2503	4493	7.68×10^{-3}	8.35×10^{-3}	132.3	SE	1.02	7.03
08/03	Non-NPF	1970	3101	9.11×10^{-3}	1.01×10^{-2}	150.8	SSE	1.11	14.23
08/06	Non-NPF	3889	5518	4.97×10^{-3}	5.36×10^{-3}	112.8	ESE	1.17	2.37
08/07	Non-NPF	1206	2043	6.80×10^{-3}	7.31×10^{-3}	123.3	ESE	1.32	5.21
08/08	Non-NPF	2307	3705	6.36×10^{-3}	6.86×10^{-3}	92.2	E	1.36	7.21

from the many point sources in the region, and not to widespread events. We also did not attempt to exclude any time periods for which the aircraft may have sampled its own exhaust, on the assumption that the crew would have avoided this wherever possible and it would appear similar to a point source in the dataset. There is some evidence of the expected negative correlation between condensation sink in the boundary layer and the occurrence of high aerosol number concentration, but no other variables show obvious trends.

3.2 Evaluation of simulated aerosol and precursor concentrations during the field campaign

Important vapor and particle concentrations were evaluated across all nine flights and are presented in aggregate in Figure 2 and for individual flights in Figure S5. The OH mixing ratio is biased high by around a factor two on 27, 28, and 29 July and reasonably well simulated on the other days for which substantial sampling was conducted around the BAO tower. Sulfur dioxide is well simulated, with the mean within 10% of observations. The mean sulfuric acid mixing ratio is biased high by around 50%, likely mostly due to the overestimate of OH and the underestimate of the concentration of larger particles (subfigure f) which are its primary sink. This overestimate in the mean sulfuric acid mixing ratio is largely driven by overestimates on 27 and 28 July. Ammonia mixing ratios are consistently underestimated by around a factor two, except on 7 and 8 August where they are well simulated. The underestimate in the mean mixing ratio is broadly consistent with other studies in Colorado (Battye et al., 2016; Eilerman et al., 2016). Total aerosol number concentration greater than around 10 nm diameter, N_{all} is well simulated, with the simulated mean matching observations to within around 10% (using the NPF mechanism from D2016). Further discussion of NPF is the subject of the following sections. The small relative underestimate in N_{all} appears

https://doi.org/10.5194/egusphere-2026-932
Preprint. Discussion started: 10 June 2026

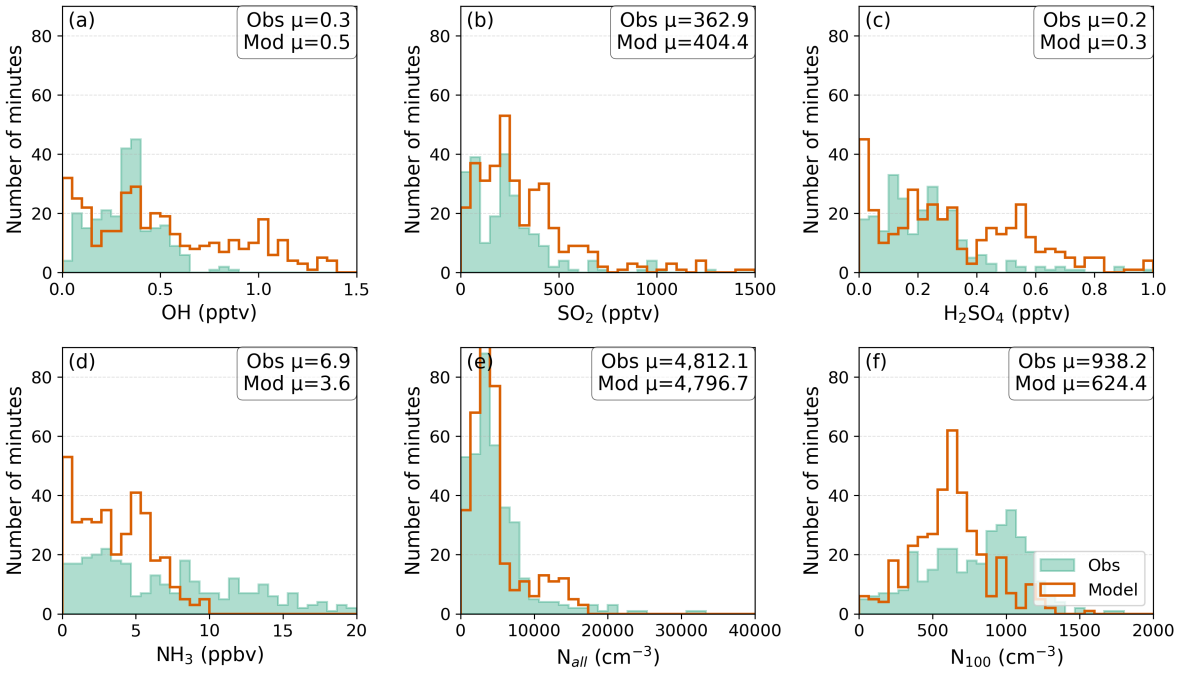

Figure 2. Concentrations of species relevant to NPF sampled by the C-130 aircraft, and simulated and interpolated onto the aircraft path, in a $0.4^\circ \times 0.4^\circ$ box around the Boulder Atmospheric Observatory tower, aggregated over all nine flights analyzed. All altitudes are included. The mean of the histograms is indicated by the μ values. The flight data are input as one-minute averages, so the y axes of the histograms count the number of minutes for which the one-minute-averaged concentrations were equal to the value on the x axes.

to be driven by the number concentration of aerosols greater than 100 nm in diameter, which is underestimated by around 30% or 300 cm^{-3}. The underestimate is likely due to a combination of missing primary emissions and missing secondary organic vapors, and is expected given that our aerosol and chemistry schemes were developed to represent global climate, not complex polluted environments.

3.3 Observations of NPF events on 31 and 27 July

In Figure 3a, we show the time evolution (in local mountain time, MDT) of the particle number size distribution on 31 July, as measured by the SMPS at the ground monitoring station (40.05° N, 105.00° W). Around 10:00 MDT, we observe notably high concentrations of N_{nuc} (~10^4 cm^{-3}) aerosol particles. Over the next 8 hours, these nucleation mode particles gradually grow into Aitken mode aerosols, with diameters ranging from 40 to 100 nm, displaying the classic 'banana' shape characteristic of a NPF event. The event follows a cold front passage that started late on 29 July and continued through 30 July, involving significant precipitation that reduced concentrations of large aerosol particles: the condensation sink on 31 July is a factor two lower than on 29 July.

https://doi.org/10.5194/egusphere-2026-932
Preprint. Discussion started: 10 June 2026

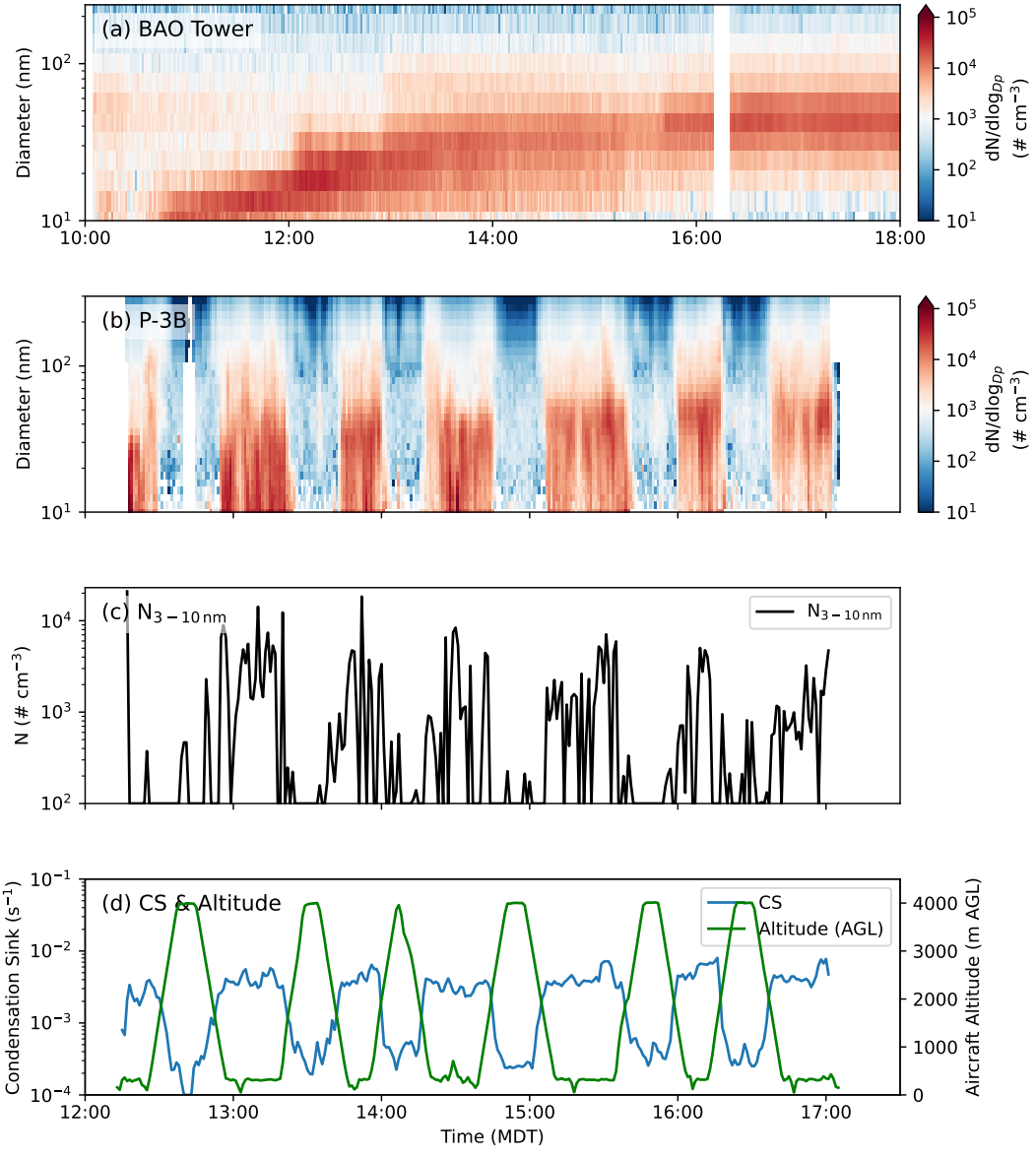

Figure 3. Particle size distributions and supporting P-3B observations on 31 July 2014. Panel (a) shows the ground-based SMPS, panel (b) the composite size distribution from the combination of the SMPS and LAS aboard the aircraft, panel (c) the nucleation-mode number concentration (N_{3-10}) derived from the two CPCs, and panel (d) the condensation sink with aircraft altitude above ground level.

https://doi.org/10.5194/egusphere-2026-932
Preprint. Discussion started: 10 June 2026

On 31 July, the NASA P-3B aircraft flew along a trajectory shown in Figure 4a, and also measured a total aerosol concentration peaking at around 10^4 cm^{-3} during the NPF event. Figures 3b, c, and d show the size distribution, nucleation-mode number concentration and condensation sink during the flight. The aircraft flew alternating legs near the surface and at around 3500 m altitude, and the higher altitude is above the NPF event. However, at all altitudes below around 1000 m, the size distribution is qualitatively consistent with the ground measurements and NPF seems to persist until at least 14:30 MDT. By this point the aircraft has traversed essentially the whole track shown in Figure 4a (the track was flown twice during the five-hour flight), so we can infer that the NPF event likely occurred over at least a 60 km$\times$40 km box centered roughly on the Boulder Atmospheric Observatory tower. The average N_{3-10nm} below an aircraft height of 2500 m is approximately 3100 cm^{-3}. The condensation sink below around 1000 m above ground level is moderate, averaging 7.0×10^{-3} s^{-1}.

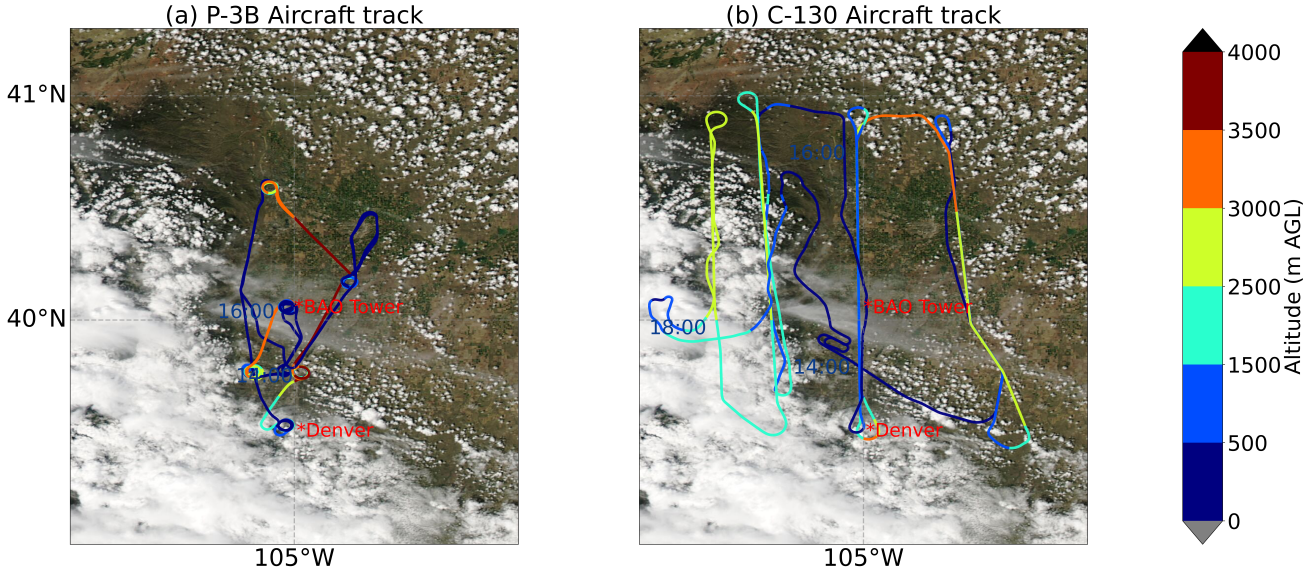

Figure 4. Flight tracks of the P-3B and C-130 during the 31 July 2014 NPF event, colored by the aircraft altitude above ground level. The background shows the Moderate Resolution Imaging Spectroradiometer (MODIS) corrected reflectance true-color image from the Aqua satellite on the day. The P3-B flew along the majority of the track shown twice during the day, keeping approximately the same pattern of altitudes between laps.

On 27 July, particle number concentrations also exceeded 10^4cm^{-3} for sustained periods. However, evidence for particle growth was less clear. The nano-SMPS next to the Boulder Atmospheric Observatory (BAO) Tower observed an 'apple' type event: large numbers of Aitken-mode aerosols, probably formed by NPF, but without growth into or out of the Aitken mode. Growth was clearer during the flight of the C-130 aircraft (Figure S6) than the P3-B (Figure S2). We investigated the C-130

https://doi.org/10.5194/egusphere-2026-932
Preprint. Discussion started: 10 June 2026

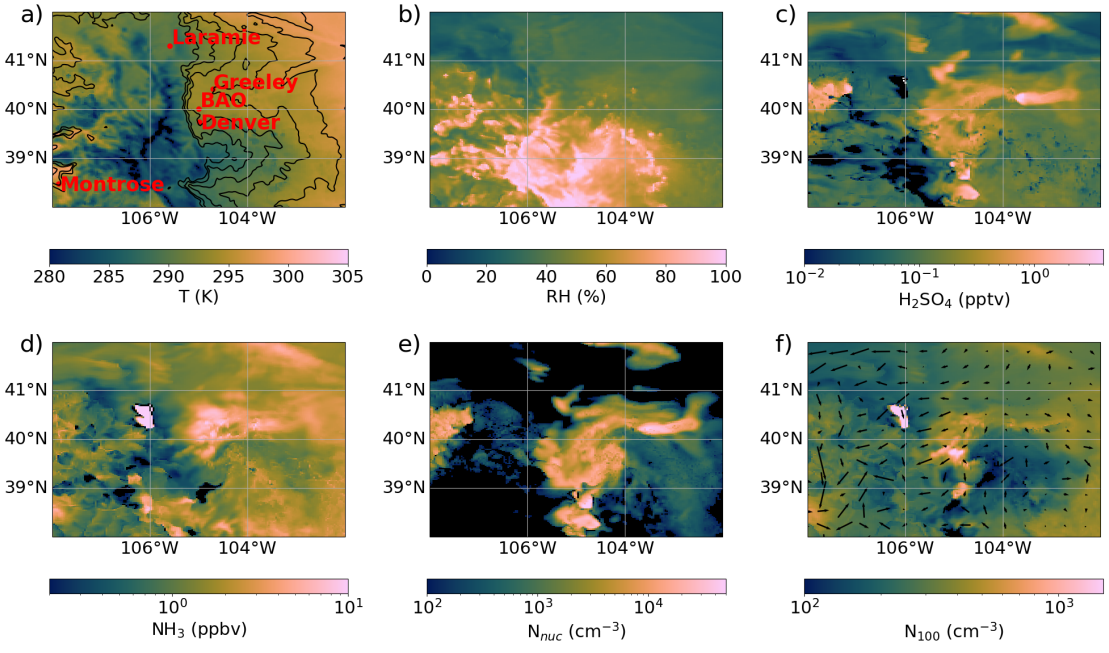

Figure 5. At 13:00 local time on 31 July 2014, simulated surface temperatures with pressure contours for pressures above 80 hPa (a), simulated relative humidity (b), simulated surface H_2SO_4 (c) and NH_3 (d) mixing ratios, and surface number concentrations of nucleation-mode (3-10 nm, e) and CCN-sized (diameter greater than 100 nm, f) aerosols. The region shown covers a slightly smaller area than the entire model domain shown in Figure 1.

measurements of this event as described in Section 3.2. Clear NPF events during daytime were also observed at the BAO tower and by the P3-B aircraft on 2nd and 6th August, but were not sampled in detail by the C-130.

3.4 Simulation of conditions for NPF on 31 and 27 July 2014

We aim to investigate whether the inorganic NPF parameterization of D2016 is able to adequately represent aerosol formation in the Colorado region. Figure 5 shows the simulated spatial patterns of precursor vapor mixing ratios, temperature, and simulated particle number concentrations during the NPF event at 13:00 local time on 31 July. The NPF event is centered on the slightly higher ground (the Palmer Divide) a little south of Denver, and extends for around 100 km into the foothills of the Front Range and up to 400 km into the plains, with some additional NPF occurring near point sources (probably coal-fired power plants, for example Pawnee Generating Station (40.22°N, 103.67°W) that are most clearly visible in the map of sulfuric acid mixing ratio, c. The southern part of the NPF event is on the western side of a cleaner area (where N_{100} concentrations are lower), south-east of Denver; this is associated with easterly winds that are forced round into southerly winds by the Front Range.

Figure 6 provides the species concentrations at 10:00 MDT on 27 July, analogous to Figure 5. This day was much more polluted than 31 July, as demonstrated in the ammonia and 100 nm aerosol concentrations (Figures 6d and f). The accumulation

https://doi.org/10.5194/egusphere-2026-932
Preprint. Discussion started: 10 June 2026

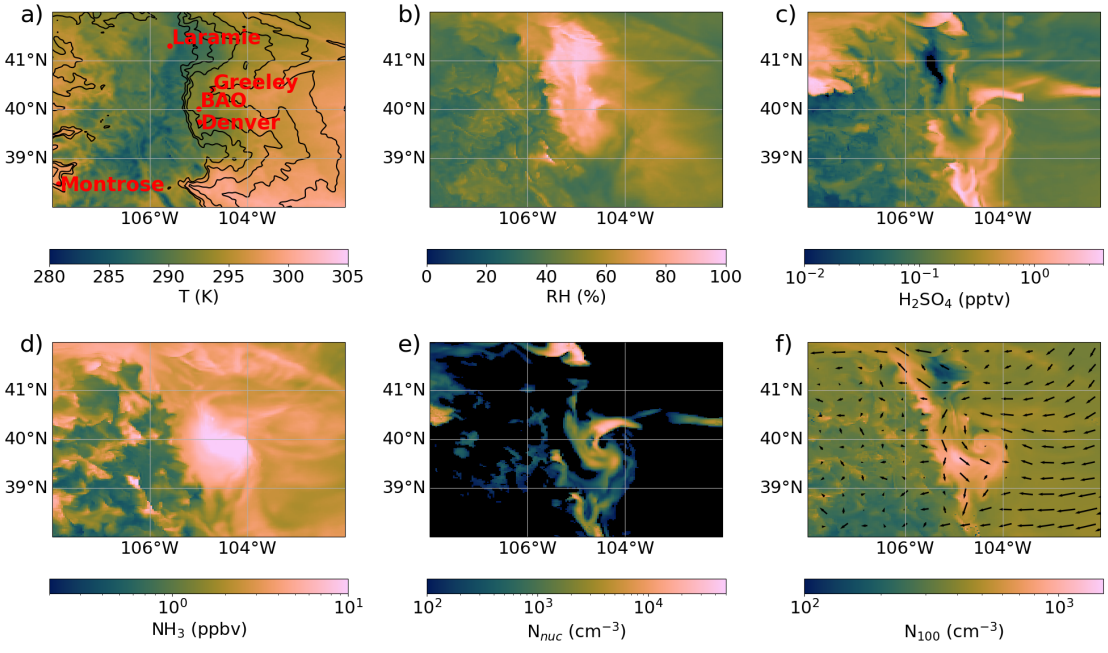

Figure 6. Simulated temperature and species concentrations, as in Figure 5, but for 10:00 local time on 27 July 2014, showing the Denver Cyclone more clearly around 39.5°N, 105°W.

of pollutants over Denver on that day due to the Denver Cyclone was studied by Vu et al. (2016). The figure shows that our model reproduces the meteorology of the Denver Cyclone reasonably (considering that this is not our primary aim). The high relative humidity associated with the cyclone observed by Vu et al. (2016) is well simulated. At 10:00 local time, we predict the center at around 39.9°N, 104.4°W, while the RAP analysis of Vu et al. (2016) predicted the center 20 km further north and 30 km further east. Sulfuric acid production and NPF are simulated in the humid air northwest of the cyclone center, likely also originating from the plume of the Pawnee coal-fired power plant. Very high levels of ammonia appear to be transported down over Denver from the Greeley area marked in the figure. The cyclone also probably transports sulfuric acid as well as moisture from the north, which then build up just south of Denver and, with the ammonia, lead to the observed NPF.

3.5 Evaluation of aerosol number concentration and size distribution on NPF days

Figure 7 shows simulated total and nucleation-mode aerosol number concentrations during the 31 July 2014 research flight of the P3-B aircraft. Corresponding figures for 27 July are shown in Figure S7. While the C-130 also measured gas-phase precursors, the P-3B aerosol data are more useful in our analysis due to the lower cut-off size of the P-3B CPC (3 nm instead of ~10 nm). The simulation with the V2002 nucleation scheme, as expected, does not reproduce the NPF occurring in the boundary layer. The simulation with the D2016 scheme reproduces the observed total aerosol number concentration within a factor of three most of the time at low altitude. Both simulations overestimate total particle concentrations in the free troposphere, above

https://doi.org/10.5194/egusphere-2026-932
Preprint. Discussion started: 10 June 2026

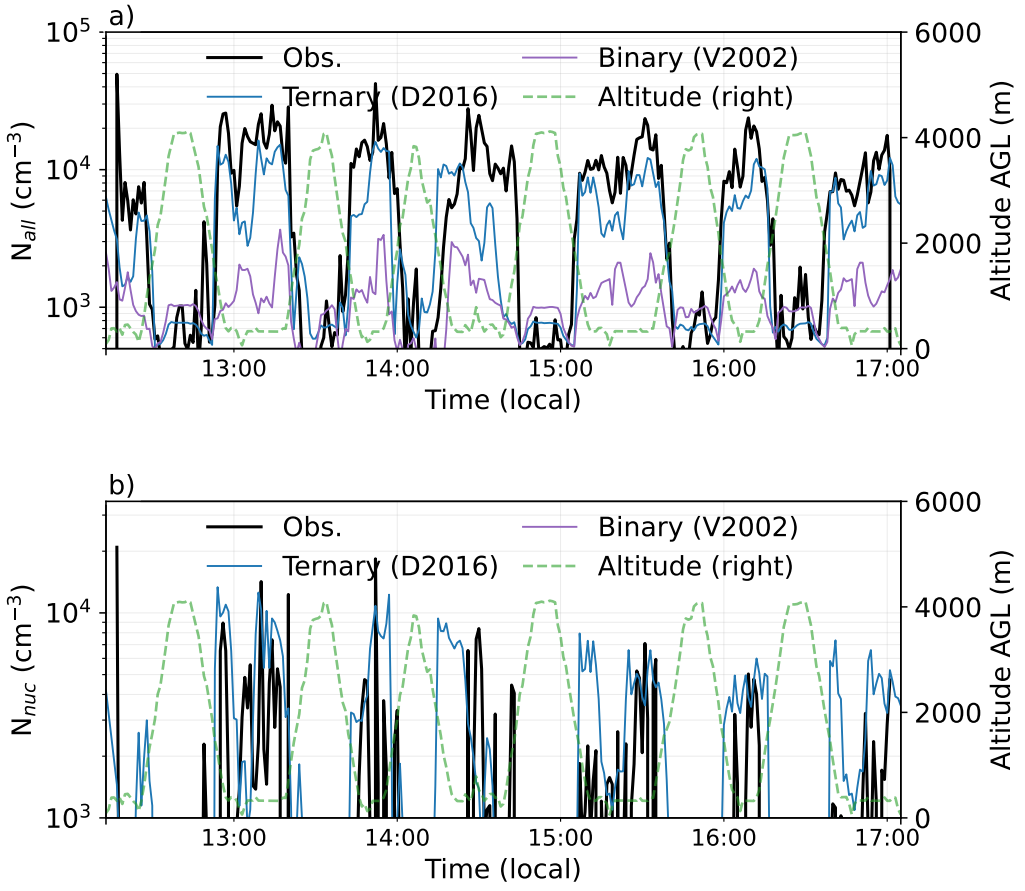

Figure 7. Total (a) and nucleation-mode (b) aerosol number concentrations observed by the P-3B on 31 July 2014 compared with the Unified Model using the D2016 ternary and V2002 binary parameterizations. Altitude above ground level is shown on the secondary axis (green dashed). Number concentrations from the C-130 aircraft are evaluated in the next section.

around 2000 m above ground level, usually by around a factor three, with the V2002 scheme predicting higher, more biased, concentrations. Yu et al. (2020) found that the V2002 scheme predicts substantially higher binary neutral formation rates than those measured in the CLOUD chamber and reported by D2016, such that the CLOUD binary ion-induced rates are still lower than the V2002 neutral rates in upper-tropospheric conditions. The nucleation-mode aerosol number concentration is simulated realistically on 31 July but substantially overpredicted on 27 July by the D2016 scheme, while essentially no nucleation-mode aerosols are formed at the altitude of the aircraft in the simulation with the V2002 scheme. The overprediction on 27 July is likely due to overestimation of sulfuric acid, as we show in the next section.

A more detailed examination of the simulated and observed size distributions for intervals during the 31 July event is provided in Figure 8. We again use the P3-B aircraft data only, because there we can produce a composite of the SMPS and

https://doi.org/10.5194/egusphere-2026-932
Preprint. Discussion started: 10 June 2026

LAS instruments, which have the same dlogDp of 0.05, while for the C-130 we would need to use the PCASP, whose size bins are not equally spaced in dlogDp. In the boundary layer, the model represents the accumulation mode well, with a slight overestimate in the number concentration but a broadly correct median diameter. This result contrasts with the finding that number concentrations greater than 100 nm are underestimated by the model on average (Figure 2f). However, while only 9 days are analyzed, it seems from Figure S5 that on cleaner days such as 31 July the simulations are in closer agreement with observations than they are on average. Consistent with the number concentrations shown in Figure 7, Figure 8 shows that the size distribution is realistically simulated below 50 nm only with the D2016 NPF parameterization (and even then the number concentration remains underestimated). Above the peak of the Aitken mode at 50 nm, the adoption of the D2016 NPF parameterization causes a small overestimate in the simulated Aitken mode number concentration. The overestimate is co-located in the size spectrum with the primary 'Aitken insoluble' mode so may result either from the NPF or from overestimated primary emissions. The observed dust number concentration in the boundary layer is very low, and is clearly overestimated by the model, but this overestimate cannot substantially affect the smaller aerosols as the dust does not act as a coagulation or condensation sink in this version of the UM. Despite the results of Valerino et al. (2017), low dust concentrations on this day are expected due to precipitation scavenging on the previous days. In the free troposphere, the model overestimates aerosol number concentration by around a factor of two in both Aitken and accumulation modes. The bias is common to both nucleation schemes and should be addressed in follow-up studies.

On 27 July, LAS data are missing, but size distributions from the simulation with the D2016 NPF parameterization are shown in Figure S8. In both the boundary layer and free troposphere on this day, the model seems to overestimate the diameter of the Aitken mode: in the boundary layer the median diameter is 21 nm in observations but 35 nm in simulations. This result suggests that the NPF event either starts too early in the simulations or that particles grow too fast. Despite the biases here and on 31 July, the model performance with the D2016 NPF parameterization is generally good - broadly comparable to that in other dedicated studies of NPF with regional models such as Zhao et al. (2020); Sullivan et al. (2018); Dong et al. (2019); Patoulias et al. (2025) - considering the complexity of the environment and the nonlinear nature of the processes we are attempting to simulate.

3.6 Attempted closure of parameterized and inferred NPF rates

It is unexpected that observed nucleation mode aerosol number concentrations in a polluted area can be explained (even approximately) by a NPF mechanism that only includes sulfuric acid, ammonia, ions and water. Thus, the simulated total and nucleation-mode number concentrations in the boundary layer shown in Figure 7 are in surprisingly good agreement with the observations. In the boundary layer, numerous experimental and modeling studies have suggested that organic molecules, amines, or iodine compounds are also important nucleation precursors (Zhang et al., 2004; Riccobono et al., 2014; Kürten et al., 2016; Zhao et al., 2024). The simultaneous measurements of sulfuric acid and ammonia concentrations on the C-130 aircraft allow us to probe the reasons for this surprisingly good agreement and to attempt a closure study to test the D2016 NPF parameterization separately from the Unified Model. Closure cannot be achieved here, partly because the NPF process is not at steady state (which we can show using simulations) and partly because the lower size cut-off of the CPC on the C-130

https://doi.org/10.5194/egusphere-2026-932
Preprint. Discussion started: 10 June 2026

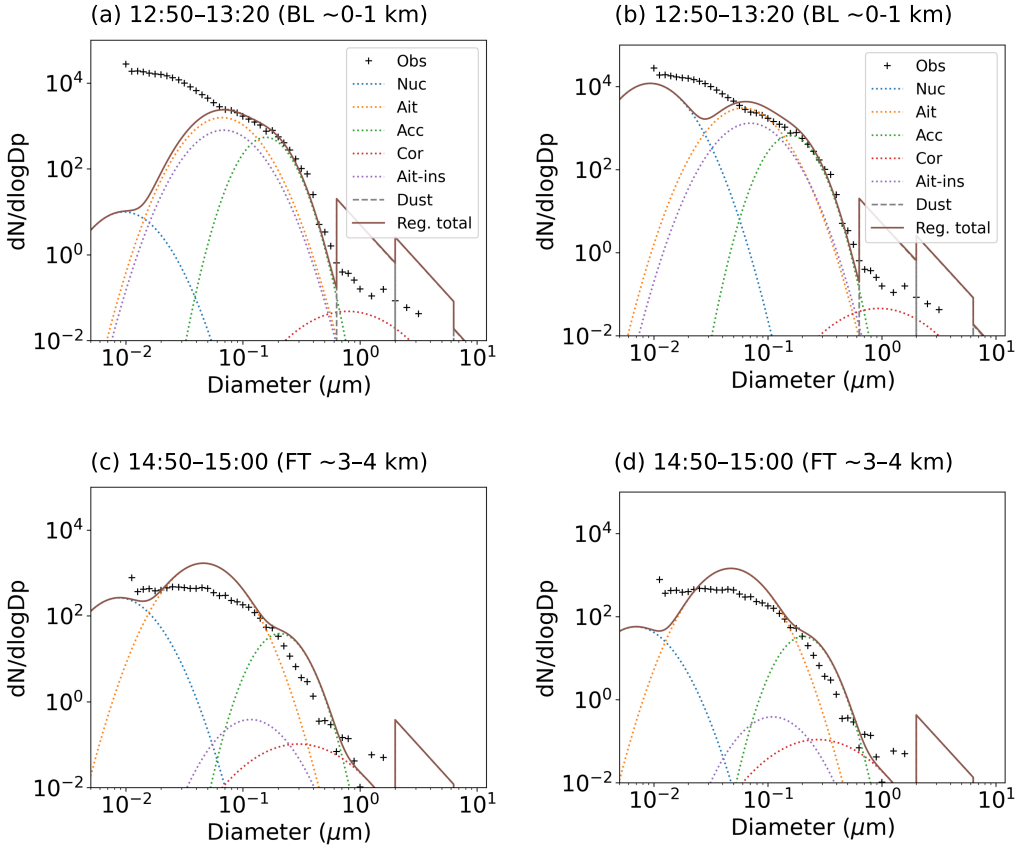

Figure 8. Size distributions on 31 July 2014 from the P3-B aircraft and simulations with Vehkamaki (a,c) and Dunne (b,d) NPF parameterizations averaged between 15:20 and 15:40 local time (in the boundary layer, top) and between 14:50 and 15:00 (in the free troposphere, bottom). The five modes of the GLOMAP aerosol scheme are shown as dashed lines. The dust concentration from its sectional representation is shown to the right of the figures. The dust mass size distribution (dM/dlogDp) is represented by logarithmically spaced bins (Woodward, 2001), so we arrive at a sawtooth pattern in the number size distribution (though as the size distribution is single-moment, only the total mass in a size section is considered by the model). .

https://doi.org/10.5194/egusphere-2026-932
Preprint. Discussion started: 10 June 2026

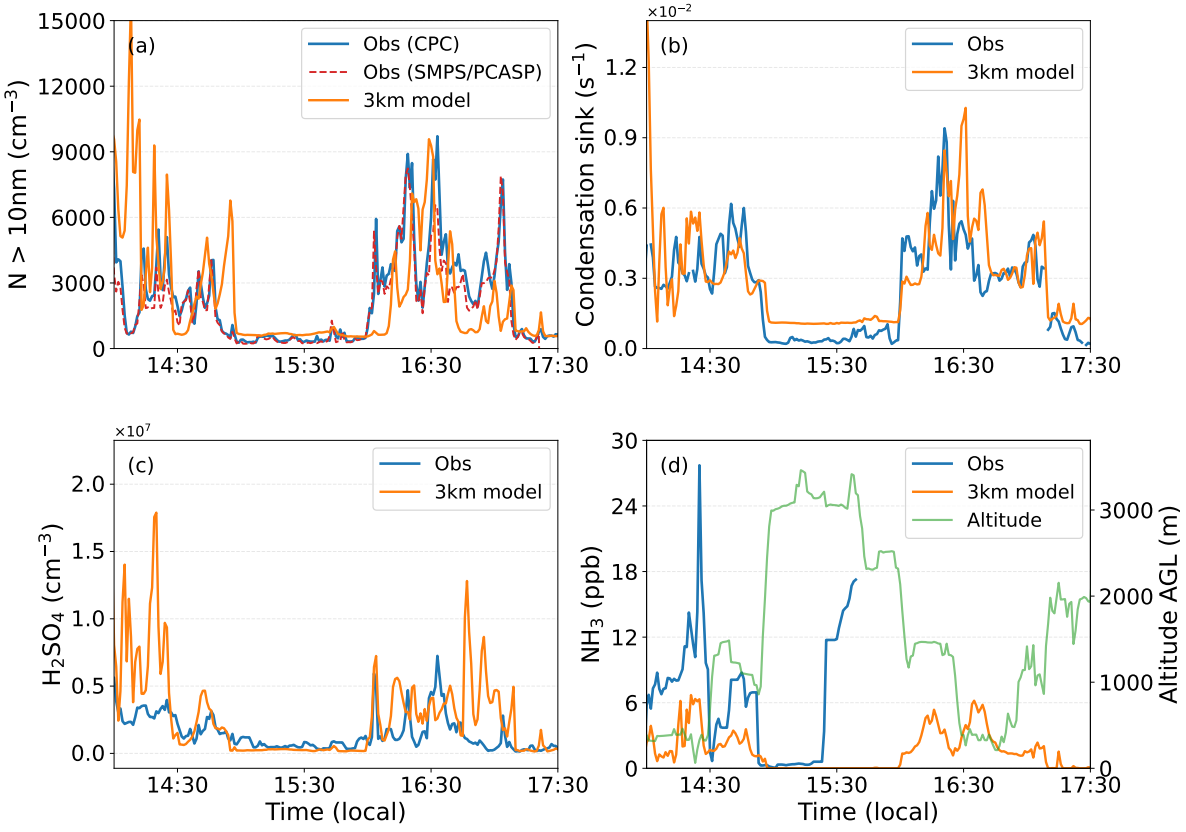

Figure 9. Particle number concentration a), condensation sink (b), sulfuric acid c), and ammonia d) concentrations observed by the C-130 aircraft, and simulated, on 31 July 2014. The entire flight is not shown since the SMPS was not operational after around 17:30. The ammonia measurement also ends shortly before 16:00 MDT.

aircraft is too high. However, the attempt helps us to illustrate the deficiencies in the NPF parameterization. Successful closure may be feasible if the process we outline here is applied to other field studies in future.

Figure 9 shows measured and simulated timeseries of the aerosol number concentration and factors controlling the NPF: sulfuric acid, ammonia, and condensation sink, on 31 July 2014. The aerosol number concentration is simulated relatively well between 14:15 and 14:45, and between 16:00 and 17:00, local time. At other times either the simulation has larger biases. The sulfuric acid concentration is usually overestimated and the ammonia concentration is underestimated, and these biases will compensate to some extent. The condensation sink appears reasonably well simulated by the model in the boundary layer (subfigure b) and this probably helps to explain the reasonably good simulation of the total number concentration.

Figure 10a shows, in green, the calculated NPF rate obtained by applying the D2016 NPF parameterization to the observed gas concentrations and the temperature and relative humidity measured by the aircraft. To perform this calculation we assumed an ion production rate of 5 ion pairs cm^{-3}s^{-1} and, as in the UM code, we calculated an ion concentration assuming a steady

https://doi.org/10.5194/egusphere-2026-932
Preprint. Discussion started: 10 June 2026

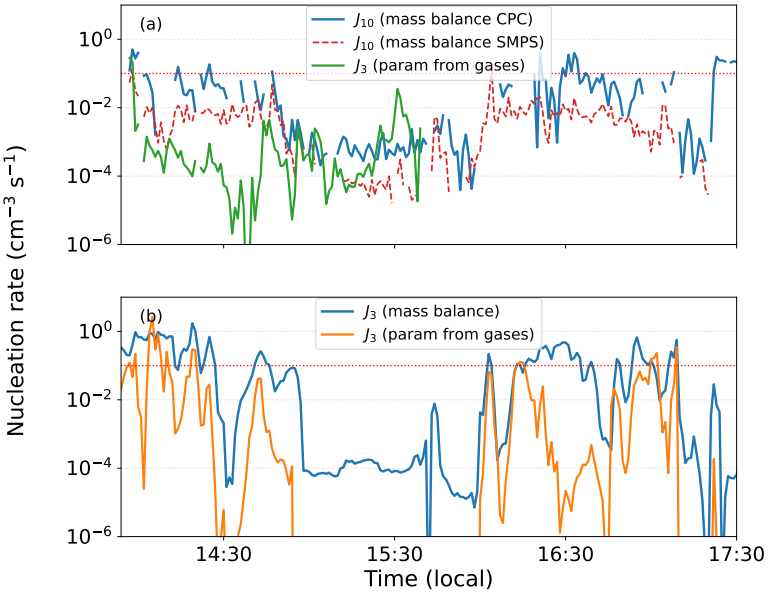

Figure 10. NPF rates calculated from a balance of nucleation-mode aerosol number concentrations between sources and sinks (see text), labelled 'mass balance' and calculated from observed gas concentrations using the Dunne et al (2016) parameterization (a), and the corresponding figure for the UM regional simulation (b), for the flight on 31 July 2014. The timeseries for the parameterized NPF rate is limited by the unavailability of ammonia data after about 15:45 MDT.

state against the condensation sink. We compared this parameterized rate timeseries of J_3 to the nucleation rate J_{10} derived from a steady state aerosol number balance (a form of the 'general dynamic equation'):

$$\frac{dN_{10}}{dt} = J_3 - \left(\sum_i K_{10i} N_i + \frac{GR}{\Delta d} \right) N_{8-12} = 0 \tag{8}$$

where J_{10} is the formation rate of 10 nm particles, $\sum K_{10i} N_i$ is the coagulation loss of ~ 10 nm diameter particles in the nucleation mode calculated using the size distributions from the SMPS and PCASP. We used the two estimates of 8-12 nm number concentration available: the difference between the CPC and the sum of the PCASP and SMPS concentrations, and the concentration in the lowest two size bins of the SMPS. Self-coagulation was verified to be negligible, and the loss due to growth out of the size range $\frac{GR}{\Delta d}$ is the growth rate GR divided by the diameter interval ($12 - 8 = 4$ nm). The GR in nm/hour was crudely parameterized as 1×10^{-7} times the sulfuric acid concentration in cm^{-3}, which roughly agrees with Stolzenburg et al. (2020). Under this assumption the losses due to growth are 20% of the losses to the coagulation sink or less, so we did not attempt to refine it by considering growth due to partitioning of nitrate or organics.

Closure remains out of reach for several reasons. First, we are comparing a parameterized J_3 to an inferred J_{10}. We cannot calculate growth from 3 nm to 10 nm diameter accurately as we lack observations of condensable vapor concentrations other than sulfuric acid, so we cannot match the diameters at which the formation rates are calculated. However, the J_{10} is a lower

https://doi.org/10.5194/egusphere-2026-932
Preprint. Discussion started: 10 June 2026

bound on the J_3 that would be obtained from the number balance approach. If the C-130 had a CPC with a lower cut-off diameter, a fairer comparison would have been possible. Related to this, the losses due to growth out of the size range in the box model may be underestimated, if nitrate and organic partitioning to these small particles greatly exceeds that of sulfuric acid. Third, we do not expect the steady-state assumption to be a good approximation: NPF is a time-varying, transient process. Fourth, in comparing the formation rate derived from the aerosol size distribution with the formation rate derived from the gas concentrations, we are assuming local homogeneity in the atmosphere: the gas concentrations do not change between the location at which the 10 nm aerosol particles were formed and the location at which they were detected. In principle, our understanding of these last two issues could be substantially improved via trajectory analysis as shown by O'Donnell et al. (2025).

To examine these sources of error in our method, we executed the same procedure for the UM simulation. We show the results in Figure 10b. There, all differences between the aerosol number balance and the parameterization should result from invalidity of either the homogeneity assumption or the steady-state assumption, as we can obtain J_3 from both number balance and parameterization for simulated data. Where the number balance and parameterization agree, we can infer the system is probably reasonably homogeneous and close to steady state. Figure 10b shows that, on this day, wherever significant nucleation is occurring ($J_3 > 0.1\,\mathrm{cm^{-3}s^{-1}}$), agreement between the methods is sometimes within 50%, but often larger discrepancies occur.

The J_{10} from our number balance is a lower bound on the 3 nm particle formation rate J_3, and this is still higher than the J_3 calculated from the measured gas concentrations with the D2016 parameterization. Therefore, despite our large uncertainties, we can infer from Figure 10a that the D2016 parameterization would not predict enough particle formation if the precursor gas concentrations matched observations. The model simulates total particle number well on this day only because it overestimates sulfuric acid concentrations. As expected, other vapors such as amines or oxidized organic molecules must be contributing to the particle formation process.

The limited availability of ammonia measurements during this flight motivated us to repeat our calculations for the flight on 27 July, when nucleation-mode aerosols are also observed. Figure S9 shows that the model substantially overestimates NPF during the first part of the C-130 flight on this day, due to a substantial overestimate in simulated sulfuric acid concentration. On this day the number balance (Figure S10) agrees even less well with the parameterized NPF rate in the simulation, with the number balance frequently overestimating the parameterization by a factor of 10. This suggests the gas concentrations are less homogeneous and/or the steady state assumption is erroneous, and the number balance calculated from observations is likely therefore also unreliable. This result could be expected from Figure 6, which shows how the Denver Cyclone leads to inhomogeneous concentrations of sulfuric acid and higher wind speeds than on 31 July (Figure 5). While the results must therefore be interpreted with caution, the D2016 parameterization again appears to significantly underestimate the NPF calculated from the number balance in observations, frequently by two orders of magnitude, again suggesting NPF cannot be explained by sulfuric and ammonia alone in reality.

https://doi.org/10.5194/egusphere-2026-932
Preprint. Discussion started: 10 June 2026

3.7 Global evaluation of surface annual mean aerosol number concentration

As we ultimately aim to better represent aerosol number concentration in global models, we tested the effect of including the D2016 parameterization on these concentrations at globally distributed surface stations. This check complements the evaluation of remote marine and high altitude aerosol number simulated with D2016 in the UM by He et al. (2025). Tables 4, 5, and 6 show the annual mean particle number concentrations observed at EBAS sites in urban and rural sites in Europe and the US, and at high altitude and remote sites, for 2015. These are compared to simulated number concentrations in our global UM simulation of 2015 for three different model configurations: NPF represented with V2002, with the binary sulfuric-acid water neutral and ion-induced NPF components of the parameterization from D2016, labeled 'D2016-binary', and with the full D2016 parameterization. The global annual mean percentage change in total aerosol number concentration when the D2016 parameterization replaces the V2002 parameterization is shown in Figure 11.

In Europe, the V2002 simulation underestimates particle concentrations at almost all sites, and particularly in urban and industrialized areas. For instance, at Annaberg-Buchholz (DE), Madrid (ES), and LE-Eisenbahnstr (DE), the modeled-to-observed ratio M/O has values ranging from 0.1 to 0.2. While this underestimation could be due in part to the low spatial resolution of the simulation ($1.9 \times 1.25°$), which might not be sufficient to capture local and inhomogeneous aerosol emissions (Kohl et al., 2023), it is also almost certainly a result of the underestimation of NPF rates at low altitudes. Indeed, surface aerosol number concentration in the simulation with V2002 NPF is most likely dominated by primary emissions rather than NPF at most sites. However, at certain remote or less populated sites, the model comes closer to reproducing observed particle concentrations, for example at Finokalia in Greece. This seems likely because of compensating errors in the model, since NPF is observed frequently there (Aktypis et al., 2024) and is unlikely to be driven only by sulfuric acid and water. The model to observation (M/O) ratios are usually similar in the D2016-binary case. This is expected since in both cases primary emissions likely dominate aerosol concentrations.

Model biases generally improve when the D2016 parameterization is used. However, large discrepancies remain, especially at urban sites. For example, in Madrid (Spain), M/O changes only marginally, from 0.10 to 0.14. At high-altitude sites like Schauinsland and Hohenpeissenberg (Germany), as well as Finokalia, this simulation modestly overestimates particle concentrations (M/O in range 1-2). Speculating based on our experience in Colorado, this seems most likely due to overestimation of sulfuric acid. In contrast, in agricultural regions like Cabauw (Netherlands) particle number concentrations remain underestimated, perhaps because of the omission of amines from the NPF mechanism.

In North America, Table: 5 shows the model exhibits relatively similar behavior to Europe. Bondville and Egbert stand out in that, unlike at most European sites at which agricultural emissions are likely important, the D2016 simulation overpredicts observations, though the factor two overprediction is relatively modest compared to the larger factor by which the V2002 simulation underpredicts.

Table 6 summarizes the performance of the model in predicting particle number concentrations across remote locations, including polar, mountainous, and forest settings. Model biases vary widely between sites. For example, at the Basic Environmental Observatory (BEO) Moussala in Bulgaria, a high-altitude mountain site, the model overestimates particle concentrations

https://doi.org/10.5194/egusphere-2026-932
Preprint. Discussion started: 10 June 2026

Table 4. Summary of global model comparisons (in M/O) across Europe for 2015, with data archived in the EBAS database. The geographical location is indicated by latitude (Lat) and longitude (Lon), and the elevation of the site above the sea surface is indicated by the altitude asl in meters (Alt). The measurement lower cutoff size for particle number concentration (cm^{-3}) is expressed in nm. The annual averages (2015) from the UM model for the nearest grid box encompassing the station are listed with 3 settings.

Site Name	Lat/Lon		Alt (m)	Cutoff size	Obser value	Model V2002	M/O	Model D2016-binary	M/O	Model D2016	M/O
Annaberg-Buchholz (DE)	50.6	13.0	545	9.4	6649	1534	0.23	1572	0.24	3837	0.58
Cabauw Zijdeweg (NL)	52.0	4.9	1.0	9.1	6324	2054	0.32	2163	0.34	4115	0.65
DD-Nord (DE)	51.1	13.7	120	4.8	10530	4343	0.41	4304	0.41	7565	0.72
DD-Winckelmannstr (DE)	51.0	13.7	112	9.4	5474	4325	0.79	4297	0.79	6071	1.11
ECO Lecce (IT)	40.3	18.1	36	9.4	5372	2747	0.51	2598	0.48	3444	0.64
Finokalia (GR)	35.3	25.7	250	8.6	1421	1278	0.90	1198	0.84	2296	1.62
Hohenpeissenberg (DE)	47.8	11.0	985	9.4	2302	1665	0.72	1677	0.73	2857	1.24
K-puszta (HU)	46.6	19.4	125	6.0	4040	2011	0.50	1924	0.48	3432	0.85
Leipzig (DE)	51.4	12.4	118	4.8	4882	1962	0.40	2037	0.42	4619	0.95
Madrid (ES)	40.5	356.3	669	14.4	11310	1088	0.10	1141	0.10	1630	0.14
Melpitz (DE)	51.5	12.9	87	4.8	7018	1962	0.28	2037	0.29	4619	0.66
Montseny (ES)	41.8	2.4	700	8.9	3056	701.0	0.23	790.1	0.26	2070	0.68
NOAK Kosetice (CZ)	49.6	15.1	534	8.6	2569	1691	0.66	1686	0.66	3528	1.37
Neuglobsow (DE)	53.1	13.0	62	9.4	2808	1212	0.43	1298	0.46	3004	1.07
OPE (FR)	48.6	5.5	392	9.7	1834	999.3	0.55	1078	0.59	2804	1.53
Prague-Suchdol (CZ)	50.1	14.4	277	5.6	6421	4339	0.68	4303	0.67	7246	1.13
SIRTA Palaiseau (FR)	48.7	2.2	162	10.0	4239	1173	0.28	1249	0.29	2471	0.58
Schauinsland (DE)	47.9	7.9	1205	9.4	1545	887.9	0.57	937.2	0.61	2362	1.53
Vielsalm (BE)	50.3	6.0	496	8.8	2082	1688	0.81	1760	0.85	4649	2.23

Table 5. Same as Table 4 but for North American sites. ASU is Appalachian State University, SGP is the Southern Great Plains Atmospheric Radiation Measurement (ARM) Observatory of the US Department of Energy.

Site Name	Lat/Lon		Alt(m)	Obser value	Model V2002	M/O	Model D2016-binary	M/O	Model D2016	M/O
ASU, Boone (NC, US)	36.21	278.31	1076	2930	1301	0.44	932.3	0.32	3866	1.32
Bondville (IL, US)	40.05	271.63	213	4095	1219	0.30	1062	0.26	6494	1.59
Egbert (ON, CA)	44.23	280.22	255	4962	1709	0.34	1152	0.23	9610	1.94
SGP, Norman (OK, US)	36.60	262.52	318	3600	856.9	0.24	851.3	0.24	2593	0.72
Trinidad Head (CA, US)	41.05	235.85	107	1526	565.5	0.37	717.7	0.47	1396	0.91

https://doi.org/10.5194/egusphere-2026-932
Preprint. Discussion started: 10 June 2026

significantly, with a M/O of 2.87 with the V2002 parameterization. The inclusion of ternary nucleation worsens this overestimation slightly to an M/O of 3.2. This overestimation likely points to either overestimated sulfuric acid or underestimated condensation sink at these relatively high altitudes. At some other high latitude sites for example Alert, Barrow, Trollhaugen, and South Pole, the V2002 simulation overestimates particle concentrations while the update to the D2016 NPF parameterization either leads to little change or reduces the overestimate.

At the highest altitude sites (BEO Moussala and South Pole), the V2002 simulation overestimates aerosol number concentration more than the ion-only simulation. This is consistent with overestimation of the NPF rates by the V2002 parameterization discussed earlier, and with the results of He et al. (2025). This effect is not visible at lower altitudes, where the D2016-binary simulation typically produces more particles than the V2002, perhaps because ion-induced NPF, which is represented in D2016-binary but not in V2002, becomes relatively more important at warmer temperatures and where radon concentrations are significant.

In contrast, at Hyytiälä (FI), a forest site, the V2002 simulation underestimates the particle number concentrations with an M/O of 0.52, and the D2016 simulation is in good agreement with observations, suggesting that ammonia plays an important role in NPF even though ammonia concentrations at Hyytiala are relatively low (Hemmilä et al., 2018). Since organic molecules are expected to be important at Hyytiälä (Petäjä et al., 2016; Lawler et al., 2018; Lehtipalo et al., 2018), it is likely the model overestimates sulfuric acid concentrations, compensating for the omission of organics from our parameterization of NPF.

Table 6. Same as Table 4 but across global remote stations.

Site Name	Setting	Lat/Lon		Alt(m)	Obser value	Model V2002	M/O	Model D2016-binary	M/O	Model D2016	M/O
BEO Moussala (BG)	Mountain	42.18	23.59	2925	542	1554	2.87	1276	2.35	1742	3.21
Hyytiälä (FI)	Forest	61.85	24.30	179	1430	744.3	0.52	882.6	0.62	1411	0.99
Sammaltunturi Pallas (FI)	Polar	67.97	24.12	565	556	348.8	0.63	480.1	0.86	598.9	1.08
Trollhaugen (NO)	Polar	-72.02	2.53	1309	154	251.0	1.63	222.7	1.45	222.2	1.44
Värriö (FI)	Polar	67.75	29.61	390	697	624.1	0.90	652.5	0.94	803.3	1.15
Zeppelin Mountain (NO)	Polar	79.90	11.86	473	161	123.6	0.77	173.3	1.08	185.8	1.15
Zugspitze (DE)	Mountain	47.41	10.98	2650	944	713.6	0.76	712.8	0.76	2476	2.62
Alert (NU, CA)	Polar	82.50	297.66	2182	205	263.5	1.29	273.2	1.33	289.3	1.41
Barrow (AK, US)	Polar	71.32	203.39	11	277	215.1	0.78	337.1	1.22	377.2	1.36
South Pole	Polar	-89.00	335.20	2841	192	203.7	1.06	145.4	0.76	148.8	0.77

Summarizing, the inclusion of ions and ammonia in the NPF parameterization in the model leads to unchanged or improved model performance at 26 of 34 sites studied, and can mitigate both underestimates and overestimates in particle number concentrations to some extent most of the time. Underestimates in agricultural regions suggest a role for other species such as amines in the NPF process. Overestimates at higher altitudes and polar sites, which are often shared between all simulations,

https://doi.org/10.5194/egusphere-2026-932
Preprint. Discussion started: 10 June 2026

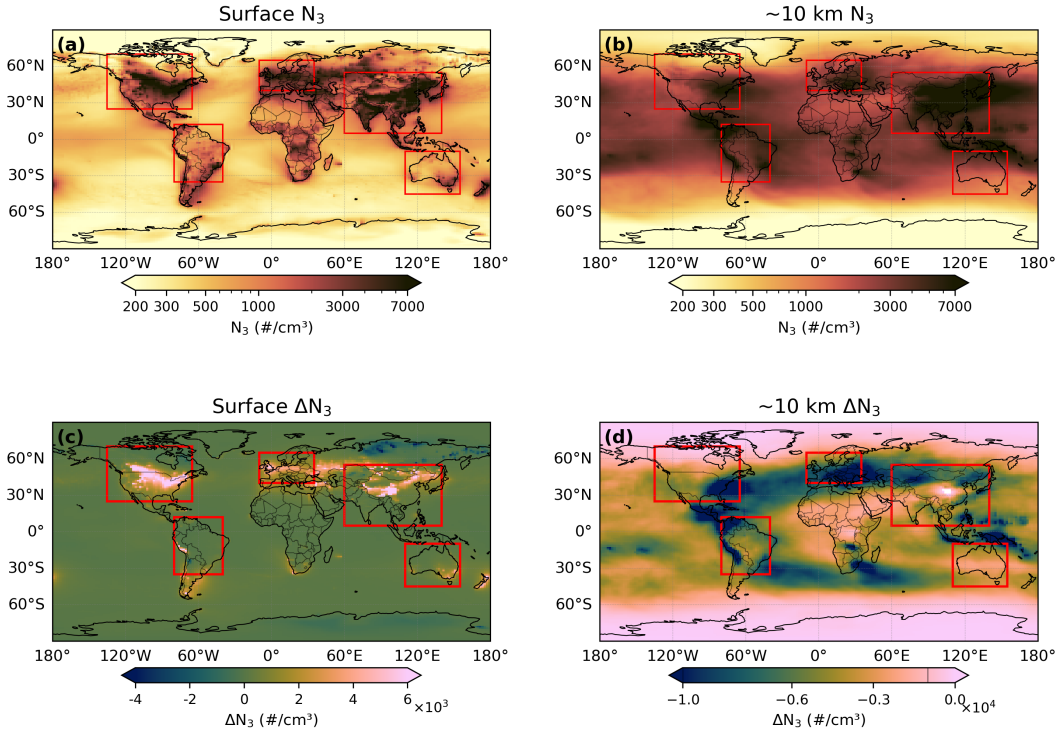

Figure 11. Number concentration of particles greater than 3 nm in diameter (N_3; a,b) with the D2016 NPF parameterization, and absolute change when the D2016 NPF parameterization replaces the V2002 parameterization (c,d) at the surface (a,c) and at ~10 km altitude (b,d). Red boxes mark regional domains over which the average N_3 and changes in N_3 are given in Table 7.

Table 7. Regional-mean N_3 simulated using the D2016 NPF parameterization and changes when this parameterization replaces that of V2002 in regions shown in Figure 11. North America is denoted NA, South America SA, Europe EU, East Asia AS, and Australia Aus.

Panel	NA	SA	EU	AS	Aus
Surface N_3	2182.30	1376.52	2951.51	3334.37	892.63
~10 km N_3	2389.77	4217.35	3165.80	6092.79	2291.23
Surface ΔN_3	1398.10	292.93	1810.24	1022.43	499.82
~10 km ΔN_3	-4164.30	-7047.58	-8016.65	-5363.99	-3639.67

https://doi.org/10.5194/egusphere-2026-932
Preprint. Discussion started: 10 June 2026

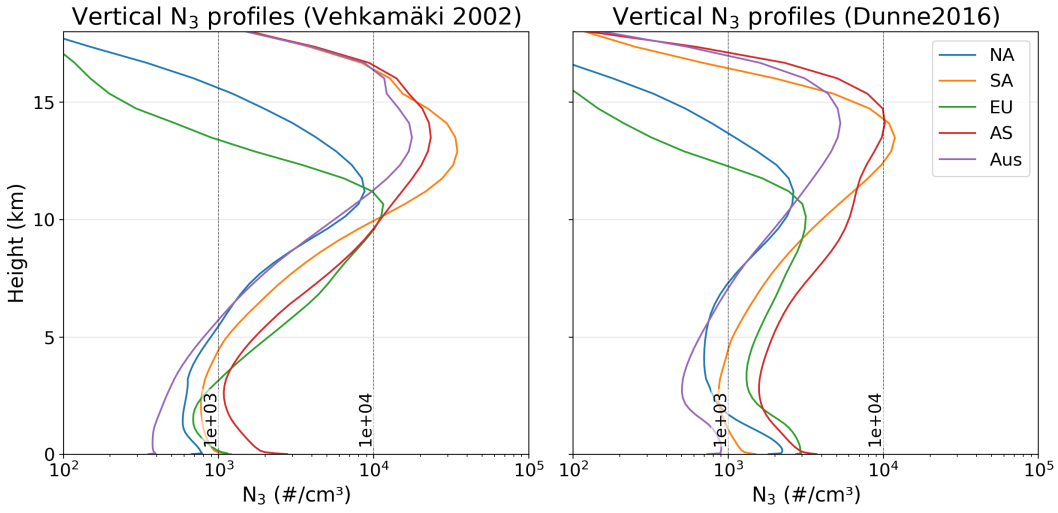

Figure 12. Vertical profiles of number concentration N_3 for the five regions shown in Figure 11. North America is denoted NA, South America SA, Europe EU, East Asia AS, and Australia Aus. The NPF parameterization differs between the two subfigures and is shown in the titles. Dashed reference lines mark 10^3 and $10^4 \mathrm{cm}^{-3}$.

suggest an overall high bias in sulfuric acid concentrations and/or a low bias in condensation sink which a more detailed evaluation could elucidate.

Figure 11 shows the global simulation of total annual mean aerosol number concentration N_3 before and after the inclusion of the D2016 NPF parameterization. At the surface, aerosol number concentration increases in polluted areas, mainly due to the role of ammonia. Some exceptions are tropical and polar remote areas where ammonia concentrations are negligible. In these areas and in the upper troposphere (subfigure d), aerosol number concentration decreases, due to mitigation of the overestimated NPF rates by the parameterization of V2002, as discussed, for example, by Yu et al. (2020) and He et al. (2025). The decreases are largest in the mid-latitudes and tropics where the absolute number concentrations (subfigure b) are highest. However, exceptionally, there is a small increase in total number concentration due to ternary NPF over central China, where number concentrations were also high already. This increase is presumably due to the high ammonia concentrations lofted to the upper troposphere by the Asian summer monsoon (Höpfner et al., 2019; Wang et al., 2022).

Figure 12 shows vertical profiles of N_3 with the two NPF parameterizations we tested. The decrease in N_3 at high altitudes when the D2016 NPF parameterization is adopted is clearly visible, while increases near the surface in Europe and North America are especially pronounced. However, the overall distribution of N_3 with altitude remains qualitatively unchanged.

4 Discussion and conclusion

A representation of NPF in atmospheric models is important for simulations of global CCN concentrations and ultimately to understand how aerosol-cloud interactions impact future climate projections. In this study we aimed to test the extent to which

https://doi.org/10.5194/egusphere-2026-932
Preprint. Discussion started: 10 June 2026

sulfuric acid and ammonia can explain aerosol number concentrations in Colorado, using observations and simulations with an updated NPF parameterization in the Unified Model. In case studies in Colorado, we succeeded, to some extent, in separating model biases in the conditions for NPF (precursor vapor concentrations, meteorological conditions and the condensation sink) from biases in the NPF parameterization. This was made possible by studying NPF events sampled by an aircraft which measured all relevant precursor species. As these events took place over a region with inhomogeneous emissions and complex topography, we needed a high-resolution regional model to understand the NPF taking place. The high resolution allowed us to associate the NPF with point sources such as coal power plants, and to simulate the meteorology of the Denver Cyclone, which creates favorable conditions for the NPF event on 27 July we studied.

We found that the NPF parameterization including ammonia could substantially improve biases in UM simulations of aerosol number concentration over land, both in the polluted Colorado region we examined in detail, and on an annual average basis at globally distributed measurement stations. During the two NPF events we analyzed in detail, on 27 and 31 July 2014, we found that the model can realistically represent the size distributions of aerosols greater than 100 nm diameter in the boundary layer while it tends to overestimate these in the free troposphere. The number concentrations of particles greater than 3 nm in diameter are within a factor two of observations for most of the 31 July flight, but more substantially overestimated, by up to a factor 10, on 27 July. On 27 July, the Aitken mode is also less well simulated (Figure S7). Both the periods of good agreement, and the periods of large bias, can be linked to good agreement, or bias, in the sulfuric acid concentrations. Ammonia concentrations are usually underpredicted by the model, though not always.

An approximate closure of nucleation-mode aerosol number concentrations via a "number balance" approach was attempted on the assumption that the source of small particles is NPF, the sink is mainly coagulation with larger particles, and the process occurs in steady state. This was used to extract NPF rates from the model and from the observations, and the rates were compared to the parameterization. The approach has serious limitations in these cases, but may have potential when aerosol number concentrations at smaller sizes (around 3 nm) are measured simultaneously with precursors. Despite these limitations, the number balance does clearly show that either the parameterization of NPF rates underestimates the rate from sulfuric acid and ammonia, or, more likely, other species participate in NPF.

The number balance also highlights the importance of accurate simulation of the sulfur cycle and especially sulfuric acid in atmospheric models: any overprediction of aerosol concentrations is most likely due to an overprediction of sulfuric acid, and biases in sulfuric acid concentration in our model can exceed 100%. Over all nine flight days we studied, sulfur dioxide was only slightly overestimated, by around 10%, and biases in sulfuric acid appear to be driven largely by biases in the concentration of hydroxyl radicals. However, despite some recent improvements in how the UM simulates the sulfur cycle (Mulcahy et al., 2023), previous experience suggests that this good simulation of sulfur dioxide may be at least partly coincidence (Ranjithkumar et al., 2021). Recent literature suggests substantial biases in sulfur dioxide in polluted regions likely exist in other models (Makroum et al., 2025), and model biases in the sulfur cycle in remote regions are also well documented (Chen et al., 2018; Wohl et al., 2024; He et al., 2025). Model evaluation would benefit from more widespread in-situ measurements of sulfur dioxide, hydroxyl radicals, and sulfuric acid with techniques that are sensitive to low concentrations (Mauldin III et al., 2001;

https://doi.org/10.5194/egusphere-2026-932
Preprint. Discussion started: 10 June 2026

Huey et al., 2004; Faloona et al., 2004; Rollins et al., 2016; Casalnuovo et al., 2025). Global studies of aerosol radiative forcing of climate also show high sensitivity to the atmospheric sulfur cycle (Carslaw et al., 2013; Stevens, 2015; Wall et al., 2022).

The conclusion that other species are also important to NPF in polluted environments is confirmed by our evaluation at globally distributed surface sites. In remote regions, the model tends to overestimate observed number concentrations, while at more polluted European and North American sites the model is much more likely to underestimate observed number concentrations, sometimes very substantially. These underestimates may be linked to averaging over large grid boxes or to primary emissions. However, there is also strong evidence from both chamber and atmospheric measurements that amines, oxygenated organic molecules, nitric acid, and iodine species participate in NPF, and our model does not yet account for these. The parameterizations available to represent these in global models are very uncertain, but modeling studies using these parameterizations produce reasonable agreement with observations and suggest these species are important (Gordon et al., 2017; Zhao et al., 2024). Representing NPF from sulfuric acid, ammonia and ions in the UM is an important first step towards representing the contributions of these other species, for example because we made ion concentrations available in the model for the first time.

Future work should include a renewed focus on the atmospheric sulfur cycle in both pristine and polluted regions. If we can improve the simulated sulfur cycle, the role of ammonia, and likely other species such as biogenic organics and amines will also likely become more critical. While the D2016 parameterization is relatively robust at the high ammonia concentrations as found in Colorado, uncertainties remain, mainly associated with the RH dependence of the D2016 NPF rates and difficulties in quantifying very low concentrations of ammonia in the CLOUD chamber. Thus there is strong motivation for additional experiments to constrain this complex system further. More confidence in the parameterized NPF rates and more testing in multiscale models should help motivate modeling centers to adopt more sophisticated parameterizations in multi-decadal climate simulations, which would enable the role of NPF in the climate system to be better understood.

Code and data availability. NASA's DISCOVER-AQ and NSF's FRAPPÉ flight campaign data is free and publicly available at https://www-air.larc.nasa.gov/cgi-bin/ArcView/discover-aq.co-2014, last access 16 February 2026. Data on particle number concentrations at globally distributed surface sites is available from EBAS, https://ebas.nilu.no, last access 16 February 2026. NASA MODIS satellite imagery as used in Figure 4 is publicly available, for example at https://worldview.earthdata.nasa.gov, last access 16 February 2026.

The data generated by the Unified Model that forms the basis for all model evaluations and results presented in this paper are archived at at https://doi.org/10.5281/zenodo.18664555 (Ding and Gordon, 2026), last access 19 Feb 2026. This includes variable outputs from the model directly on selected model levels, as well interpolated data needed to reproduce the figures in this paper. The python scripts we used to create the figures are also included in the repository. The source code for the Unified Model used in this study is free to use. However, software for this research is not publicly available due to licensing restrictions, but is available to signatories of the Met Office Software license. Full descriptions of the software, including the specific configurations used in this study, can be found in the text of this article and in articles cited therein. Software is stored in the Met Office Science Repository Service at https://code.metoffice.gov.uk/trac/home. To apply for a license, go to https://www.metoffice.gov.uk/research/approach/collaboration/momentum-partnership. The Rose and Cylc software used to drive the Unified Model are publicly available at https://github.com/metomi/rose and https://cylc.github.io/ respectively.

Simulation identifiers are as follows:

https://doi.org/10.5194/egusphere-2026-932
Preprint. Discussion started: 10 June 2026

- u-ds161: NUMAC simulation over the field campaign period with NPF represented according to V2002
- u-ds160: NUMAC simulation over the field campaign period with NPF represented according to Dunne et al. (2016)
- u-cz749: 1-year global simulation with NPF represented according to Vehkamäki et al. (2002)
- u-cz606: 1-year global simulation with NPF represented according to Dunne et al. (2016) with binary NPF only.
- u-cz594: 1-year global simulation with NPF represented according to Dunne et al. (2016)

Author contributions. HD and HG formulated the idea of the paper. HD, PG and HG set up and ran simulations. HD implemented the parameterization, with contributions from HG, DO'N and XCH. RLM, JNS and JO made measurements and helped interpret observation data. HD and HG analyzed data and wrote the paper with comments and suggestions from all co-authors.

Competing interests. The authors declare that no competing interests are present.

Acknowledgements. We thank the DISCOVER-AQ and FRAPPÉ science teams for the execution of the field campaigns. This research was supported by the National Aeronautics & Space Administration (NASA) under the NASA ROSES grant number 80NSSC19K0949. HG additionally acknowledges support from the US National Science Foundation under grant number 2442132. XCH acknowledges support from Research Council of Finland grants no. 359331, 349659, 371185. Model simulations are material produced using Met Office software. Figures 1, 4, 11 and 12 and Tables 3-7 were produced from simulation data using code that was in large part written by ChatGPT. The relevant scripts are archived with our other analysis scripts, see Data Availability, and checked for accuracy by the authors. This work used the Extreme Science and Engineering Discovery Environment (XSEDE), which is supported by the NSF Award ACI-1928147, at the Pittsburgh Supercomputing Center (PSC). This work also used Bridges-2 at the PSC through allocation atm200005p from the Advanced Cyberinfrastructure Coordination Ecosystem: Services & Support (ACCESS) program, which is supported by National Science Foundation grants #2138259, #2138286, #2138307, #2137603, and #2138296. The EBAS database has largely been funded by the UN-ECE CLRTAP (EMEP), AMAP and through NILU internal resources. Specific developments have been possible due to projects like EUSAAR (EU-FP5)(EBAS web interface), EBAS-Online (Norwegian Research Council INFRA) (upgrading of database platform) and HTAP (European Commission DG-ENV)(import and export routines to build a secondary repository in support of www.htap.org). A large number of specific projects have supported development of data and meta data reporting schemes in dialog with data providers (EU)(CREATE, ACTRIS and others). For a complete list of programmes and projects for which EBAS serves as a database, please consult the information box in the Framework filter of the web interface. These are all highly acknowledged for their support. Work at Lawrence Livermore National Laboratory (LLNL) was performed under the auspices of the US DOE by LLNL under contract no. DE-AC52-07NA27344 (LLNL IM: LLNL-JRNL-2016054).

https://doi.org/10.5194/egusphere-2026-932
Preprint. Discussion started: 10 June 2026

References

Aktypis, A., Kaltsonoudis, C., Patoulias, D., Kalkavouras, P., Matrali, A., Vasilakopoulou, C. N., Kostenidou, E., Florou, K., Kalivitis, N., Bougiatioti, A., Eleftheriadis, K., Vratolis, S., Gini, M. I., Kouras, A., Samara, C., Lazaridis, M., Chatoutsidou, S.-E., Mihalopoulos, N., and Pandis, S. N.: Significant spatial gradients in new particle formation frequency in Greece during summer, Atmospheric Chemistry and Physics, 24, 65–84, https://doi.org/10.5194/acp-24-65-2024, 2024.

Archibald, A. T., O'Connor, F. M., Abraham, N. L., Archer-Nicholls, S., Chipperfield, M. P., Dalvi, M., Folberth, G. A., Dennison, F., Dhomse, S. S., Griffiths, P. T., Hardacre, C., Hewitt, A. J., Hill, R. S., Johnson, C. E., Keeble, J., Köhler, M. O., Morgenstern, O., Mulcahy, J. P., Ordóñez, C., Pope, R. J., Rumbold, S. T., Russo, M. R., Savage, N. H., Sellar, A., Stringer, M., Turnock, S. T., Wild, O., and Zeng, G.: Description and evaluation of the UKCA stratosphere–troposphere chemistry scheme (StratTrop vn 1.0) implemented in UKESM1, Geoscientific Model Development, 13, 1223–1266, https://doi.org/10.5194/gmd-13-1223-2020, 2020.

Bahreini, R., Ahmadov, R., McKeen, S. A., Vu, K. T., Dingle, J. H., Apel, E. C., Blake, D. R., Blake, N., Campos, T. L., Cantrell, C., Flocke, F., Fried, A., Gilman, J. B., Hills, A. J., Hornbrook, R. S., Huey, G., Kaser, L., Lerner, B. M., Mauldin, R. L., Meinardi, S., Montzka, D. D., Richter, D., Schroeder, J. R., Stell, M., Tanner, D., Walega, J., Weibring, P., and Weinheimer, A.: Sources and characteristics of summertime organic aerosol in the Colorado Front Range: perspective from measurements and WRF-Chem modeling, Atmospheric Chemistry and Physics, 18, 8293–8312, https://doi.org/10.5194/acp-18-8293-2018, 2018.

Ball, S. M., Hanson, D. R., Eisele, F. L., and McMurry, P. H.: Laboratory studies of particle nucleation: Initial results for H2SO4, H2O, and NH3 vapors, Journal of Geophysical Research: Atmospheres, 104, 23 709–23 718, https://doi.org/https://doi.org/10.1029/1999JD900411, 1999.

Baranizadeh, E., Murphy, B. N., Julin, J., Falahat, S., Reddington, C. L., Arola, A., Ahlm, L., Mikkonen, S., Fountoukis, C., Patoulias, D., Minikin, A., Hamburger, T., Laaksonen, A., Pandis, S. N., Vehkamäki, H., Lehtinen, K. E. J., and Riipinen, I.: Implementation of state-of-the-art ternary new-particle formation scheme to the regional chemical transport model PMCAMx-UF in Europe, Geoscientific Model Development, 9, 2741–2754, https://doi.org/10.5194/gmd-9-2741-2016, 2016.

Battye, W. H., Bray, C. D., Aneja, V. P., Tong, D., Lee, P., and Tang, Y.: Evaluating ammonia (NH3) predictions in the NOAA National Air Quality Forecast Capability (NAQFC) using in situ aircraft, ground-level, and satellite measurements from the DISCOVER-AQ Colorado campaign, Atmospheric Environment, 140, 342–351, https://doi.org/10.1016/J.ATMOSENV.2016.06.021, 2016.

Bellouin, N., Mann, G. W., Woodhouse, M. T., Johnson, C., Carslaw, K. S., and Dalvi, M.: Impact of the modal aerosol scheme GLOMAP-mode on aerosol forcing in the Hadley Centre Global Environmental Model, Atmospheric Chemistry and Physics, 13, 3027–3044, https://doi.org/10.5194/acp-13-3027-2013, 2013.

Bellouin, N., Quaas, J., Gryspeerdt, E., Kinne, S., Stier, P., Watson-Parris, D., Boucher, O., Carslaw, K. S., Christensen, M., Daniau, A.-L., Dufresne, J.-L., Feingold, G., Fiedler, S., Forster, P., Gettelman, A., Haywood, J. M., Lohmann, U., Malavelle, F., Mauritsen, T., McCoy, D. T., Myhre, G., Mülmenstädt, J., Neubauer, D., Possner, A., Rugenstein, M., Sato, Y., Schulz, M., Schwartz, S. E., Sourdeval, O., Storelvmo, T., Toll, V., Winker, D., and Stevens, B.: Bounding Global Aerosol Radiative Forcing of Climate Change, Reviews of Geophysics, 58, e2019RG000 660, https://doi.org/https://doi.org/10.1029/2019RG000660, e2019RG000660 10.1029/2019RG000660, 2020.

Best, M. J., Pryor, M., Clark, D. B., Rooney, G. G., Essery, R. L. H., Ménard, C. B., Edwards, J. M., Hendry, M. A., Porson, A., Gedney, N., Mercado, L. M., Sitch, S., Blyth, E., Boucher, O., Cox, P. M., Grimmond, C. S. B., and Harding, R. J.: The Joint UK Land

https://doi.org/10.5194/egusphere-2026-932
Preprint. Discussion started: 10 June 2026

Environment Simulator (JULES), model description – Part 1: Energy and water fluxes, Geoscientific Model Development, 4, 677–699, https://doi.org/10.5194/gmd-4-677-2011, 2011.

Boucher, O., Randall, D., Artaxo, P., Bretherton, C., Feingold, G., Forster, P., Kerminen, V.-M., Y., K., Liao, H., Lohmann, U., Rasch, P., Satheesh, S., Sherwood, S., Stevens, B., and Zhang, X.: Clouds and Aerosols, p. 571–658, Cambridge University Press, https://doi.org/10.1017/CBO9781107415324.016, 2014.

Boy, M., Karl, T., Turnipseed, A., Mauldin, R. L., Kosciuch, E., Greenberg, J., Rathbone, J., Smith, J., Held, A., Barsanti, K., Wehner, B., Bauer, S., Wiedensohler, A., Bonn, B., Kulmala, M., and Guenther, A.: New particle formation in the Front Range of the Colorado Rocky Mountains, Atmospheric Chemistry and Physics, 8, 1577–1590, https://doi.org/10.5194/acp-8-1577-2008, 2008.

Brasseur, G. and Chatel, A.: Modelling of stratospheric ions: a first attempt, Ann. Geophys. (Eur. Geophys. Soc.), 1, 173–185, 1983.

Brock, C. A., Hamill, P., Wilson, J. C., Jonsson, H. H., and Chan, K. R.: Particle Formation in the Upper Tropical Troposphere: A Source of Nuclei for the Stratospheric Aerosol, Science, 270, 1650–1653, https://doi.org/10.1126/science.270.5242.1650, 1995.

Bush, M., Boutle, I., Edwards, J., Finnenkoetter, A., Franklin, C., Hanley, K., Jayakumar, A., Lewis, H., Lock, A., Mittermaier, M., Mohandas, S., North, R., Porson, A., Roux, B., Webster, S., and Weeks, M.: The second Met Office Unified Model–JULES Regional Atmosphere and Land configuration, RAL2, Geoscientific Model Development, 16, 1713–1734, https://doi.org/10.5194/gmd-16-1713-2023, 2023.

Carslaw, K. S., Lee, L. A., Reddington, C. L., Mann, G. W., and Pringle, K. J.: The magnitude and sources of uncertainty in global aerosol, Faraday Discussions, 165, 495–512, https://doi.org/10.1039/c3fd00043e, 2013.

Casalnuovo, D. A., Cheng, D., Romero-Flores, M., Montesinos-Castellanos, A., and Jen, C. N.: A reactive condensation particle counter for measuring atmospherically relevant concentrations of sulfuric acid, Aerosol Science and Technology, 59, 794–805, https://doi.org/10.1080/02786826.2025.2459705, 2025.

Chen, M., Titcombe, M., Jiang, J., Jen, C., Kuang, C., Fischer, M. L., Eisele, F. L., Siepmann, J. I., Hanson, D. R., Zhao, J., and McMurry, P. H.: No Title, 109, https://doi.org/10.1073/pnas.1210285109, 2012.

Chen, Q., Sherwen, T., Evans, M., and Alexander, B.: DMS oxidation and sulfur aerosol formation in the marine troposphere: a focus on reactive halogen and multiphase chemistry, Atmospheric Chemistry and Physics, 18, 13 617–13 637, https://doi.org/10.5194/acp-18-13617-2018, 2018.

Clark, D. B., Mercado, L. M., Sitch, S., Jones, C. D., Gedney, N., Best, M. J., Pryor, M., Rooney, G. G., Essery, R. L. H., Blyth, E., Boucher, O., Harding, R. J., Huntingford, C., and Cox, P. M.: The Joint UK Land Environment Simulator (JULES), model description – Part 2: Carbon fluxes and vegetation dynamics, Geoscientific Model Development, 4, 701–722, https://doi.org/10.5194/gmd-4-701-2011, 2011.

Clarke, A. D.: Atmospheric nuclei in the Pacific midtroposphere: Their nature, concentration, and evolution, Journal of Geophysical Research, 98, 20 633, https://doi.org/10.1029/93JD00797, 1993.

Cooper, W.: NCAR/RAF Processing Algorithms, https://rpubs.com/cooperwilliama/RAFProcessingAlgorithms, accessed: 2025-06-16, 2022.

Dal Maso, M., Kulmala, M., Riipinen, I., Wagner, R., Hussein, T., Aalto, P. P., and Lehtinen, K. E.: Formation and growth of fresh atmospheric aerosols: eight years of aerosol size distribution data from SMEAR II, Hyytiälä, Finland, Boreal environment research, 10, 323, 2005.

Denier van der Gon, H., Hendriks, C., Kuenen, J., Segers, A., and Visschedijk, A.: Description of current temporal emission patterns and sensitivity of predicted AQ for temporal emission patterns. TNO Rep. EU FP7 MACC Deliverable Rep. D_DEMIS_1. 3, 22 pp, 2011.

Ding, H. and Gordon, H.: Supporting code and data for Multiscale atmospheric modeling suggests ammonia is necessary but not sufficient to explain new particle formation in the Colorado boundary layer, https://doi.org/10.5281/zenodo.18664555, 2026.

https://doi.org/10.5194/egusphere-2026-932
Preprint. Discussion started: 10 June 2026

Dong, C., Matsui, H., Spak, S., Kalafut-Pettibone, A., and Stanier, C.: Impacts of new particle formation on short-term meteorology and air quality as determined by the NPF-explicit WRF-Chem in the Midwestern United States, Aerosol and Air Quality Research, 19, 204–220, 2019.

Dunne, E. M., Gordon, H., KÃŒrten, A., Almeida, J., Duplissy, J., Williamson, C., Ortega, I. K., Pringle, K. J., Adamov, A., Baltensperger, U., Barmet, P., Benduhn, F., Bianchi, F., Breitenlechner, M., Clarke, A., Curtius, J., Dommen, J., Donahue, N. M., Ehrhart, S., Flagan, R. C., Franchin, A., Guida, R., Hakala, J., Hansel, A., Heinritzi, M., Jokinen, T., Kangasluoma, J., Kirkby, J., Kulmala, M., Kupc, A., Lawler, M. J., Lehtipalo, K., Makhmutov, V., Mann, G., Mathot, S., Merikanto, J., Miettinen, P., Nenes, A., Onnela, A., Rap, A., Reddington, C. L. S., Riccobono, F., Richards, N. A. D., Rissanen, M. P., Rondo, L., Sarnela, N., Schobesberger, S., Sengupta, K., Simon, M., SipilÃ, M., Smith, J. N., Stozkhov, Y., TomÃ©, A., TrÃ¶stl, J., Wagner, P. E., Wimmer, D., Winkler, P. M., Worsnop, D. R., and Carslaw, K. S.: Global atmospheric particle formation from CERN CLOUD measurements, Science, 354, 1119–1124, https://doi.org/10.1126/science.aaf2649, 2016.

Ehrhart, S., Dunne, E. M., Manninen, H. E., Nieminen, T., Lelieveld, J., and Pozzer, A.: Two new submodels for the Modular Earth Submodel System (MESSy): New Aerosol Nucleation (NAN) and small ions (IONS) version 1.0, Geoscientific Model Development, 11, 4987–5001, https://doi.org/10.5194/gmd-11-4987-2018, 2018.

Eilerman, S. J., Peischl, J., Neuman, J. A., Ryerson, T. B., Aikin, K. C., Holloway, M. W., Zondlo, M. A., Golston, L. M., Pan, D., Floerchinger, C., and Herndon, S.: Characterization of Ammonia, Methane, and Nitrous Oxide Emissions from Concentrated Animal Feeding Operations in Northeastern Colorado, Environmental Science & Technology, 50, 10 885–10 893, https://doi.org/10.1021/acs.est.6b02851, pMID: 27662008, 2016.

Faloona, I. C., Tan, D., Lesher, R. L., Hazen, N. L., Frame, C. L., Simpas, J. B., Harder, H., Martinez, M., Di Carlo, P., Ren, X., and Brune, W. H.: A laser-induced fluorescence instrument for detecting tropospheric OH and HO2: Characteristics and calibration, Journal of Atmospheric Chemistry, 47, 139–167, https://doi.org/10.1023/B:JOCH.0000021036.53185.0e, 2004.

Field, P. R., Hill, A., Shipway, B., Furtado, K., Wilkinson, J., Miltenberger, A., Gordon, H., Grosvenor, D. P., Stevens, R., and Van Weverberg, K.: Implementation of a double moment cloud microphysics scheme in the UK met office regional numerical weather prediction model, Quarterly Journal of the Royal Meteorological Society, 149, 703–739, https://doi.org/https://doi.org/10.1002/qj.4414, 2023.

Flocke, F., Pfister, G., Crawford, J. H., Pickering, K. E., Pierce, G., Bon, D., and Reddy, P.: Air Quality in the Northern Colorado Front Range Metro Area: The Front Range Air Pollution and Photochemistry Éxperiment (FRAPPÉ), Journal of Geophysical Research: Atmospheres, 125, e2019JD031 197, https://doi.org/https://doi.org/10.1029/2019JD031197, e2019JD031197 2019JD031197, 2020.

Forster, P., Storelvmo, T., Armour, K., Collins, W., Dufresne, J.-L., Frame, D., Lunt, D. J., Mauritsen, T., Palmer, M. D., Watanabe, M., Wild, M., and Zhang, X.: The Earth's energy budget, climate feedbacks, and climate sensitivity, in: Climate Change 2021: The Physical Science Basis. Contribution of Working Group I to the Sixth Assessment Report of the Intergovernmental Panel on Climate Change, edited by Masson-Delmotte, V., Zhai, P., Pirani, A., Connors, S. L., Péan, C., Berger, S., Caud, N., Chen, Y., Goldfarb, L., Gomis, M. I., Huang, M., Leitzell, K., Lonnoy, E., Matthews, J. B. R., Maycock, T. K., Waterfield, T., Yelekçi, O., Yu, R., and Zhou, B., pp. 923–1054, Cambridge University Press, Cambridge, United Kingdom and New York, NY, USA, https://doi.org/10.1017/9781009157896.001, 2021.

Ghosh, P., Boutle, I., Field, P., Hill, A., Jones, A., Mazoyer, M., Evans, K. J., Mahajan, S., Kang, H.-G., Xu, M., Zhang, W., Asch, N., and Gordon, H.: High sensitivity of simulated fog properties to parameterized aerosol activation in case studies from ParisFog, Atmospheric Chemistry and Physics, 25, 11 129–11 156, https://doi.org/10.5194/acp-25-11129-2025, 2025.

https://doi.org/10.5194/egusphere-2026-932
Preprint. Discussion started: 10 June 2026

Giuffrida, E., Johnson, K., Tatro, T., Zuidema, P., and Gordon, H.: Biomass burning aerosol radiative effects in the Southeast Atlantic depend strongly on meteorological forcing method, Atmospheric Chemistry and Physics, 25, 14 879–14 907, https://doi.org/10.5194/acp-25-14879-2025, 2025.

Gordon, H., Kirkby, J., Baltensperger, U., Bianchi, F., Breitenlechner, M., Curtius, J., Dias, A., Dommen, J., Donahue, N. M., Dunne, E. M., Duplissy, J., Ehrhart, S., Flagan, R. C., Frege, C., Fuchs, C., Hansel, A., Hoyle, C. R., Kulmala, M., Kürten, A., Lehtipalo, K., Makhmutov, V., Molteni, U., Rissanen, M. P., Stozkhov, Y., Tröstl, J., Tsagkogeorgas, G., Wagner, R., Williamson, C., Wimmer, D., Winkler, P. M., Yan, C., and Carslaw, K. S.: Causes and importance of new particle formation in the present-day and preindustrial atmospheres, Journal of Geophysical Research: Atmospheres, 122, 8739–8760, https://doi.org/10.1002/2017JD026844, 2017.

Gordon, H., Field, P. R., Abel, S. J., Barrett, P., Bower, K., Crawford, I., Cui, Z., Grosvenor, D. P., Hill, A. A., Taylor, J., Wilkinson, J., Wu, H., and Carslaw, K. S.: Development of aerosol activation in the double-moment Unified Model and evaluation with CLARIFY measurements, Atmospheric Chemistry and Physics, 20, 10 997–11 024, https://doi.org/10.5194/acp-20-10997-2020, 2020.

Gordon, H., Carslaw, K. S., Hill, A. A., Field, P. R., Abraham, N. L., Beyersdorf, A., Corr-Limoges, C., Ghosh, P., Hemmings, J., Jones, A. C., Sanchez, C., Wang, X., and Wilkinson, J.: NUMAC: Description of the Nested Unified Model With Aerosols and Chemistry, and Evaluation With KORUS-AQ Data, Journal of Advances in Modeling Earth Systems, 15, e2022MS003 457, https://doi.org/https://doi.org/10.1029/2022MS003457, e2022MS003457 2022MS003457, 2023.

He, X.-C., Abraham, N. L., Ding, H., Russo, M. R., Grosvenor, D. P., Ge, Y., Wang, X., Jones, A. C., Campuzano-Jost, P., Nault, B., Kupc, A., Blake, D., Jimenez, J. L., Williamson, C. J., Carslaw, K. S., Weber, J., Archibald, A. T., and Gordon, H.: Evaluation of UKESM aerosol size and composition using ATom measurements indicates missing marine aerosol formation mechanisms, EGUsphere, 2025, 1–71, https://doi.org/10.5194/egusphere-2025-3700, 2025.

Hemmilä, M., Hellén, H., Virkkula, A., Makkonen, U., Praplan, A. P., Kontkanen, J., Ahonen, L., Kulmala, M., and Hakola, H.: Amines in boreal forest air at SMEAR II station in Finland, Atmospheric Chemistry and Physics, 18, 6367–6380, https://doi.org/10.5194/acp-18-6367-2018, 2018.

Höpfner, M., Ungermann, J., Borrmann, S., Wagner, R., Spang, R., Riese, M., Stiller, G., Appel, O., Batenburg, A. M., Bucci, S., Cairo, F., Dragoneas, A., Friedl-Vallon, F., Hünig, A., Johansson, S., Krasauskas, L., Legras, B., Leisner, T., Mahnke, C., Möhler, O., Molleker, S., Müller, R., Neubert, T., Orphal, J., Preusse, P., Rex, M., Saathoff, H., Stroh, F., Weigel, R., and Wohltmann, I.: Ammonium nitrate particles formed in upper troposphere from ground ammonia sources during Asian monsoons, Nature geoscience, 12, 608–612, 2019.

Hoppel, W. A. and Frick, G. M.: Ion-Aerosol Attachment Coefficients and the Steady-State Charge Distribution on Aerosols in a Bipolar Ion Environment, Aerosol Science and Technology, 5, 1–21, https://doi.org/10.1080/02786828608959073, 1986.

Huang, G., Brook, R., Crippa, M., Janssens-Maenhout, G., Schieberle, C., Dore, A., Guizzardi, D., Muntean, M., Schaaf, E., and Friedrich, R.: Speciation of anthropogenic emissions of non-methane volatile organic compounds: a global gridded data set for 1970–2012, Atmospheric Chemistry and Physics, 17, 7683–7701, https://doi.org/10.5194/acp-17-7683-2017, 2017.

Huey, L., Tanner, D., Slusher, D., Dibb, J., Arimoto, R., Chen, G., Davis, D., Buhr, M., Nowak, J., Mauldin, R., Eisele, F., and Kosciuch, E.: CIMS measurements of HNO3 and SO2 at the South Pole during ISCAT 2000, Atmospheric Environment, 38, 5411–5421, https://doi.org/https://doi.org/10.1016/j.atmosenv.2004.04.037, antarctic Atmospheric Chemistry: ISCAT 2000, 2004.

Jones, A. C., Hill, A., Remy, S., Abraham, N. L., Dalvi, M., Hardacre, C., Hewitt, A. J., Johnson, B., Mulcahy, J. P., and Turnock, S. T.: Exploring the sensitivity of atmospheric nitrate concentrations to nitric acid uptake rate using the Met Office's Unified Model, Atmospheric Chemistry and Physics, 21, 15 901–15 927, https://doi.org/10.5194/acp-21-15901-2021, 2021.

https://doi.org/10.5194/egusphere-2026-932
Preprint. Discussion started: 10 June 2026

Kerminen, V.-M. and Kulmala, M.: Analytical formulae connecting the "real" and the "apparent" nucleation rate and the nuclei number concentration for atmospheric nucleation events, Journal of Aerosol Science, 33, 609–622, https://doi.org/10.1016/S0021-8502(01)00194-X, 2002.

Kirkby, J., Curtius, J., Almeida, J., Dunne, E., Duplissy, J., Ehrhart, S., Franchin, A., Gagné, S., Ickes, L., Kürten, A., Kupc, A., Metzger, A., Riccobono, F., Rondo, L., Schobesberger, S., Tsagkogeorgas, G., Wimmer, D., Amorim, A., Bianchi, F., Breitenlechner, M., David, A., Dommen, J., Downard, A., Ehn, M., Flagan, R. C., Haider, S., Hansel, A., Hauser, D., Jud, W., Junninen, H., Kreissl, F., Kvashin, A., Laaksonen, A., Lehtipalo, K., Lima, J., Lovejoy, E. R., Makhmutov, V., Mathot, S., Mikkilä, J., Minginette, P., Mogo, S., Nieminen, T., Onnela, A., Pereira, P., Petäjä, T., Schnitzhofer, R., Seinfeld, J. H., Sipilä, M., Stozhkov, Y., Stratmann, F., Tomé, A., Vanhanen, J., Viisanen, Y., Vrtala, A., Wagner, P. E., Walther, H., Weingartner, E., Wex, H., Winkler, P. M., Carslaw, K. S., Worsnop, D. R., Baltensperger, U., and Kulmala, M.: Role of sulphuric acid, ammonia and galactic cosmic rays in atmospheric aerosol nucleation, Nature, 476, 429–435, https://doi.org/10.1038/nature10343, 2011.

Kohl, M., Lelieveld, J., Chowdhury, S., Ehrhart, S., Sharma, D., Cheng, Y., Tripathi, S. N., Sebastian, M., Pandithurai, G., Wang, H., and Pozzer, A.: Numerical simulation and evaluation of global ultrafine particle concentrations at the Earth's surface, EGUsphere, https://doi.org/10.5194/egusphere-2023-317, [preprint], 2023.

Kürten, A., Bianchi, F., Almeida, J., Kupiainen-Määttä, O., Dunne, E. M., Duplissy, J., Williamson, C., Barmet, P., Breitenlechner, M., Dommen, J., Donahue, N. M., Flagan, R. C., Franchin, A., Gordon, H., Hakala, J., Hansel, A., Heinritzi, M., Ickes, L., Jokinen, T., Kangasluoma, J., Kim, J., Kirkby, J., Kupc, A., Lehtipalo, K., Leiminger, M., Makhmutov, V., Onnela, A., Ortega, I. K., Petäjä, T., Praplan, A. P., Riccobono, F., Rissanen, M. P., Rondo, L., Schnitzhofer, R., Schobesberger, S., Smith, J. N., Steiner, G., Stozhkov, Y., Tomé, A., Tröstl, J., Tsagkogeorgas, G., Wagner, P. E., Wimmer, D., Ye, P., Baltensperger, U., Carslaw, K., Kulmala, M., and Curtius, J.: Experimental particle formation rates spanning tropospheric sulfuric acid and ammonia abundances, ion production rates, and temperatures, Journal of Geophysical Research: Atmospheres, 121, 12,377–12,400, https://doi.org/10.1002/2015JD023908, 2016.

Lawler, M. J., Rissanen, M. P., Ehn, M., Mauldin III, R. L., Sarnela, N., Sipilä, M., and Smith, J. N.: Evidence for Diverse Biogeochemical Drivers of Boreal Forest New Particle Formation, Geophysical Research Letters, 45, 2038–2046, https://doi.org/https://doi.org/10.1002/2017GL076394, 2018.

Lehtipalo, K., Yan, C., Dada, L., Bianchi, F., Xiao, M., Wagner, R., Stolzenburg, D., Ahonen, L. R., Amorim, A., Baccarini, A., Bauer, P. S., Baumgartner, B., Bergen, A., Bernhammer, A.-K., Breitenlechner, M., Brilke, S., Buchholz, A., Mazon, S. B., Chen, D., Chen, X., Dias, A., Dommen, J., Draper, D. C., Duplissy, J., Ehn, M., Finkenzeller, H., Fischer, L., Frege, C., Fuchs, C., Garmash, O., Gordon, H., Hakala, J., He, X., Heikkinen, L., Heinritzi, M., Helm, J. C., Hofbauer, V., Hoyle, C. R., Jokinen, T., Kangasluoma, J., Kerminen, V.-M., Kim, C., Kirkby, J., Kontkanen, J., Kürten, A., Lawler, M. J., Mai, H., Mathot, S., Mauldin, R. L., Molteni, U., Nichman, L., Nie, W., Nieminen, T., Ojdanic, A., Onnela, A., Passananti, M., Petäjä, T., Piel, F., Pospisilova, V., Quelever, L. L. J., Rissanen, M. P., Rose, C., Sarnela, N., Schallhart, S., Schuchmann, S., Sengupta, K., Simon, M., Sipilä, M., Tauber, C., Tomé, A., Tröstl, J., Vaisanen, O., Vogel, A. L., Volkamer, R., Wagner, A. C., Wang, M., Weitz, L., Wimmer, D., Ye, P., Ylisirna, A., Zha, Q., Carslaw, K. S., Curtius, J., Donahue, N. M., Flagan, R. C., Hansel, A., Riipinen, I., Virtanen, A., Winkler, P. M., Baltensperger, U., Kulmala, M., and Worsnop, D. R.: Multicomponent new particle formation from sulfuric acid, ammonia, and biogenic vapors, Science Advances, 4, eaau5363, https://doi.org/10.1126/sciadv.aau5363, 2018.

Lock, A. P., Brown, A. R., Bush, M. R., Martin, G. M., and Smith, R. N. B.: A New Boundary Layer Mixing Scheme. Part I: Scheme Description and Single-Column Model Tests, Monthly Weather Review, 128, 3187–3199, https://doi.org/10.1175/1520-0493(2000)128<3187:ANBLMS>2.0.CO;2, 2000.

https://doi.org/10.5194/egusphere-2026-932
Preprint. Discussion started: 10 June 2026

Määttänen, A., Merikanto, J., Henschel, H., Duplissy, J., Makkonen, R., Ortega, I. K., and Vehkamäki, H.: New Parameterizations for Neutral and Ion-Induced Sulfuric Acid-Water Particle Formation in Nucleation and Kinetic Regimes, Journal of Geophysical Research: Atmospheres, 123, 1269–1296, https://doi.org/10.1002/2017JD027429, 2018.

Makroum, I., Jöckel, P., Dameris, M., Theys, N., and De Leeuw, J.: Evaluation of atmospheric sulfur dioxide simulated with the EMAC (version 2.55) Chemistry-Climate Model using satellite and ground-based observations, EGUsphere, 2025, 1–45, https://doi.org/10.5194/egusphere-2025-3915, 2025.

Mann, G. W., Carslaw, K. S., Spracklen, D. V., Ridley, D. A., Manktelow, P. T., Chipperfield, M. P., Pickering, S. J., and Johnson, C. E.: Description and evaluation of GLOMAP-mode: a modal global aerosol microphysics model for the UKCA composition-climate model, Geoscientific Model Development, 3, 519–551, https://doi.org/10.5194/gmd-3-519-2010, 2010.

Manners, J., Edwards, J. M., Hill, P., and Thelen, J.-C.: SOCRATES (Suite Of Community RAdiative Transfer codes based on Edwards and Slingo) Technical Guide, https://code.metoffice.gov.uk/trac/socrates, 2017.

Mao, J., Jiang, L., Feng, Z., Li, J., Zhu, Y., Qin, M., Guo, S., Hu, M., and Hu, J.: Enhancing particle number concentration modelling accuracy in China by incorporating various nucleation parameterization schemes into the CMAQ version 5.3.2 model, Geoscientific Model Development, 18, 8423–8438, https://doi.org/10.5194/gmd-18-8423-2025, 2025.

Mauldin III, R. L., Eisele, F. L., Tanner, D. J., Kosciuch, E., Shetter, R., Lefer, B., Hall, S. R., Nowak, J. B., Buhr, M., Chen, G., Wang, P., and Davis, D.: Measurements of OH, H2SO4, and MSA at the South Pole during ISCAT, Geophysical Research Letters, 28, 3629–3632, https://doi.org/https://doi.org/10.1029/2000GL012711, 2001.

McMurry, P. and Friedlander, S.: New particle formation in the presence of an aerosol, Atmospheric Environment (1967), 13, 1635–1651, https://doi.org/10.1016/0004-6981(79)90322-6, 1979.

Merikanto, J., Spracklen, D. V., Mann, G. W., Pickering, S. J., and Carslaw, K. S.: Impact of nucleation on global CCN, Atmospheric Chemistry and Physics, 9, 8601–8616, https://doi.org/10.5194/acp-9-8601-2009, 2009.

Metzger, A., Verheggen, B., Dommen, J., Duplissy, J., Prevot, A. S. H., Weingartner, E., Riipinen, I., Kulmala, M., Spracklen, D. V., Carslaw, K. S., and Baltensperger, U.: Evidence for the role of organics in aerosol particle formation under atmospheric conditions, Proceedings of the National Academy of Sciences, 107, 6646–6651, https://doi.org/10.1073/pnas.0911330107, 2010.

Mohnen, V.: Electrical Processes in Atmospheres, D. Steinkopff, Darmstadt, pp. 1–17, 1977.

Mulcahy, J., Johnson, C., Jones, C., Povey, A., Scott, C., Sellar, A., Turnock, S., Woodhouse, M., Andrews, M., Bellouin, N., Browse, J., Carslaw, K., Dalvi, M., Folberth, G., Glover, M., Grosvenor, D., Hardacre, C., Hill, R., Johnson, B., Jones, A., Kipling, Z., Mann, G., Mollard, J., O'Connor, F., Palmieri, J., Reddington, C., Rumbold, S., Richardson, M., Schutgens, N. A., Stier, P., Stringer, M., Tang, Y., Walton, J., Woodward, S., and Yool, A.: Description and evaluation of aerosol in UKESM1 and HadGEM3-GC3.1 CMIP6 historical simulations, Geoscientific Model Development Discussions, pp. 1–59, https://doi.org/10.5194/gmd-2019-357, 2020.

Mulcahy, J. P., Jones, C. G., Rumbold, S. T., Kuhlbrodt, T., Dittus, A. J., Blockley, E. W., Yool, A., Walton, J., Hardacre, C., Andrews, T., Bodas-Salcedo, A., Stringer, M., de Mora, L., Harris, P., Hill, R., Kelley, D., Robertson, E., and Tang, Y.: UKESM1.1: development and evaluation of an updated configuration of the UK Earth System Model, Geosci. Model Dev., 16, 1569–1600, https://doi.org/10.5194/gmd-16-1569-2023, 2023.

Nair, A. A., Yu, F., and Luo, G.: The importance of ammonia for springtime atmospheric new particle formation and aerosol number abundance over the United States, Science of The Total Environment, 863, 160 756, https://doi.org/https://doi.org/10.1016/j.scitotenv.2022.160756, 2023.

https://doi.org/10.5194/egusphere-2026-932
Preprint. Discussion started: 10 June 2026

Ortega, J., Snider, J. R., Smith, J. N., and Reeves, J. M.: Comparison of aerosol measurement systems during the 2016 airborne ARISTO campaign, Aerosol Science and Technology, 53, 871–885, https://doi.org/10.1080/02786826.2019.1610554, 2019.

O'Donnell, S. E., Croft, B., Ford, B., June, N. A., Kuang, C., Singh, A., Chang, R. Y.-W., Collins, D. R., Hakala, S., Jathar, S. H., Paasonen, P., Shrivastava, M., Smith, J. N., and Pierce, J. R.: Going Off Grid: A Comparative Study of the Lagrangian and Eulerian Perspectives of New Particle Formation Events, Journal of Geophysical Research: Atmospheres, 130, e2025JD043 713, https://doi.org/https://doi.org/10.1029/2025JD043713, e2025JD043713 2025JD043713, 2025.

Patoulias, D., Florou, K., and Pandis, S. N.: Sensitivity of predicted ultrafine particle size distributions in Europe to different nucleation rate parameterizations using PMCAMx-UF v2.2, Geoscientific Model Development, 18, 1103–1118, https://doi.org/10.5194/gmd-18-1103-2025, 2025.

Petäjä, T., O'Connor, E. J., Moisseev, D., Sinclair, V. A., Manninen, A. J., Väänänen, R., von Lerber, A., Thornton, J. A., Nicoll, K., Petersen, W., Chandrasekar, V., Smith, J. N., Winkler, P. M., Krüger, O., Hakola, H., Timonen, H., Brus, D., Laurila, T., Asmi, E., Riekkola, M.-L., Mona, L., Massoli, P., Engelmann, R., Komppula, M., Wang, J., Kuang, C., Bäck, J., Virtanen, A., Levula, J., Ritsche, M., and Hickmon, N.: BAECC: A Field Campaign to Elucidate the Impact of Biogenic Aerosols on Clouds and Climate, Bulletin of the American Meteorological Society, 97, 1909 – 1928, https://doi.org/10.1175/BAMS-D-14-00199.1, 2016.

Pfister, G. G., Reddy, P. J., Barth, M. C., Flocke, F. F., Fried, A., Herndon, S. C., Sive, B. C., Sullivan, J. T., Thompson, A. M., Yacovitch, T. I., Weinheimer, A. J., and Wisthaler, A.: Using Observations and Source-Specific Model Tracers to Characterize Pollutant Transport During FRAPPÉ and DISCOVER-AQ, Journal of Geophysical Research: Atmospheres, 122, 10,510–10,538, https://doi.org/https://doi.org/10.1002/2017JD027257, 2017.

Pierce, J. R. and Adams, P. J.: Efficiency of cloud condensation nuclei formation from ultrafine particles, Atmospheric Chemistry and Physics, 7, 1367–1379, https://doi.org/10.5194/acp-7-1367-2007, 2007.

Ranjithkumar, A., Gordon, H., Williamson, C., Rollins, A., Pringle, K., Kupc, A., Abraham, N. L., Brock, C., and Carslaw, K.: Constraints on global aerosol number concentration, SO2 and condensation sink in UKESM1 using ATom measurements, Atmospheric Chemistry and Physics, 21, 4979–5014, https://doi.org/10.5194/acp-21-4979-2021, 2021.

Riccobono, F., Schobesberger, S., Scott, C. E., Dommen, J., Ortega, I. K., Rondo, L., Almeida, J., Amorim, A., Bianchi, F., Breitenlechner, M., David, A., Downard, A., Dunne, E. M., Duplissy, J., Ehrhart, S., Flagan, R. C., Franchin, A., Hansel, A., Junninen, H., Kajos, M., Keskinen, H., Kupc, A., Kurten, A., Kvashin, A. N., Laaksonen, A., Lehtipalo, K., Makhmutov, V., Mathot, S., Nieminen, T., Onnela, A., Petaja, T., Praplan, A. P., Santos, F. D., Schallhart, S., Seinfeld, J. H., Sipila, M., Spracklen, D. V., Stozhkov, Y., Stratmann, F., Tome, A., Tsagkogeorgas, G., Vaattovaara, P., Viisanen, Y., Vrtala, A., Wagner, P. E., Weingartner, E., Wex, H., Wimmer, D., Carslaw, K. S., Curtius, J., Donahue, N. M., Kirkby, J., Kulmala, M., Worsnop, D. R., and Baltensperger, U.: Oxidation Products of Biogenic Emissions Contribute to Nucleation of Atmospheric Particles, Science, 344, 717–721, https://doi.org/10.1126/science.1243527, 2014.

Rollins, A. W., Thornberry, T. D., Ciciora, S. J., McLaughlin, R. J., Watts, L. A., Hanisco, T. F., Baumann, E., Giorgetta, F. R., Bui, T. V., Fahey, D. W., and Gao, R.-S.: A laser-induced fluorescence instrument for aircraft measurements of sulfur dioxide in the upper troposphere and lower stratosphere, Atmospheric Measurement Techniques, 9, 4601–4613, https://doi.org/10.5194/amt-9-4601-2016, 2016.

Schobesberger, S., Junninen, H., Bianchi, F., Lonn, G., Ehn, M., Lehtipalo, K., Dommen, J., Ehrhart, S., Ortega, I. K., Franchin, A., Nieminen, T., Riccobono, F., Hutterli, M., Duplissy, J., Almeida, J., Amorim, A., Breitenlechner, M., Downard, A. J., Dunne, E. M., Flagan, R. C., Kajos, M., Keskinen, H., Kirkby, J., Kupc, A., Kurten, A., Kurten, T., Laaksonen, A., Mathot, S., Onnela, A., Praplan, A. P., Rondo, L., Santos, F. D., Schallhart, S., Schnitzhofer, R., Sipila, M., Tome, A., Tsagkogeorgas, G., Vehkamaki, H., Wimmer, D., Baltensperger, U., Carslaw, K. S., Curtius, J., Hansel, A., Petaja, T., Kulmala, M., Donahue, N. M., and Worsnop, D. R.: Molecular understanding of

https://doi.org/10.5194/egusphere-2026-932
Preprint. Discussion started: 10 June 2026

atmospheric particle formation from sulfuric acid and large oxidized organic molecules, Proceedings of the National Academy of Sciences, 110, 17 223–17 228, https://doi.org/10.1073/pnas.1306973110, 2013.

Schutgens, N. A. J., Gryspeerdt, E., Weigum, N., Tsyro, S., Goto, D., Schulz, M., and Stier, P.: Will a perfect model agree with perfect observations? The impact of spatial sampling, Atmos. Chem. Phys., 16, 6335–6353, https://doi.org/10.5194/acp-16-6335-2016, publisher: Copernicus Publications, 2016.

Scott, W. and Cattell, F.: Vapor pressure of ammonium sulfates, Atmospheric Environment, 13, 307–317, https://doi.org/https://doi.org/10.1016/0004-6981(79)90174-4, 1979.

Sellar, A. A., Jones, C. G., Mulcahy, J. P., Tang, Y., Yool, A., Wiltshire, A., O'Connor, F. M., Stringer, M., Hill, R., Palmieri, J., Woodward, S., de Mora, L., Kuhlbrodt, T., Rumbold, S. T., Kelley, D. I., Ellis, R., Johnson, C. E., Walton, J., Abraham, N. L., Andrews, M. B., Andrews, T., Archibald, A. T., Berthou, S., Burke, E., Blockley, E., Carslaw, K., Dalvi, M., Edwards, J., Folberth, G. A., Gedney, N., Griffiths, P. T., Harper, A. B., Hendry, M. A., Hewitt, A. J., Johnson, B., Jones, A., Jones, C. D., Keeble, J., Liddicoat, S., Morgenstern, O., Parker, R. J., Predoi, V., Robertson, E., Siahaan, A., Smith, R. S., Swaminathan, R., Woodhouse, M. T., Zeng, G., and Zerroukat, M.: UKESM1: Description and Evaluation of the U.K. Earth System Model, Journal of Advances in Modeling Earth Systems, 11, 4513–4558, https://doi.org/10.1029/2019MS001739, 2019.

Semeniuk, K. and Dastoor, A.: Current state of aerosol nucleation parameterizations for air-quality and climate modeling New Particle Formation : Nucleation and Initial Growth, Atmospheric Environment, 179, 77–106, https://doi.org/10.1016/j.atmosenv.2018.01.039, 2018.

Shao, X., Wang, M., Dong, X., Liu, Y., Shen, W., Arnold, S. R., Regayre, L. A., Andreae, M. O., Pöhlker, M. L., Jo, D. S., Yue, M., and Carslaw, K. S.: Global modeling of aerosol nucleation with a semi-explicit chemical mechanism for highly oxygenated organic molecules (HOMs), Atmospheric Chemistry and Physics, 24, 11 365–11 389, https://doi.org/10.5194/acp-24-11365-2024, 2024.

Smith, R. N.: A scheme for predicting layer clouds and their water content in a general circulation model, Quarterly Journal of the Royal Meteorological Society, 116, 435–460, https://doi.org/10.1002/qj.49711649210, 1990.

Stevens, B.: Rethinking the lower bound on aerosol radiative forcing, Journal of Climate, 28, 4794–4819, https://doi.org/10.1175/JCLI-D-14-00656.1, 2015.

Stolzenburg, D., Simon, M., Ranjithkumar, A., Kürten, A., Lehtipalo, K., Gordon, H., Ehrhart, S., Finkenzeller, H., Pichelstorfer, L., Nieminen, T., et al.: Enhanced growth rate of atmospheric particles from sulfuric acid, Atmos. Chem. Phys., 20, 7359–7372, https://doi.org/10.5194/acp-20-7359-2020, 2020.

Stolzenburg, D., Cai, R., Blichner, S. M., Kontkanen, J., Zhou, P., Makkonen, R., Kerminen, V.-M., Kulmala, M., Riipinen, I., and Kangasluoma, J.: Atmospheric nanoparticle growth, Reviews of Modern Physics, 95, 045 002, 2023.

Sullivan, R. C., Crippa, P., Matsui, H., Leung, L. R., Zhao, C., Thota, A., and Pryor, S. C.: New particle formation leads to cloud dimming, npj Climate and Atmospheric Science, 1, 9, https://doi.org/10.1038/s41612-018-0019-7, 2018.

Telford, P. J., Braesicke, P., Morgenstern, O., and Pyle, J. A.: Technical Note: Description and assessment of a nudged version of the new dynamics Unified Model, Atmospheric Chemistry and Physics, 8, 1701–1712, https://doi.org/10.5194/acp-8-1701-2008, 2008.

Tevlin, A. G., Li, Y., Collett, J. L., McDuffie, E. E., Fischer, E. V., and Murphy, J. G.: Tall Tower Vertical Profiles and Diurnal Trends of Ammonia in the Colorado Front Range, Journal of Geophysical Research: Atmospheres, 122, 12,468–12,487, https://doi.org/https://doi.org/10.1002/2017JD026534, 2017.

Thuburn, J.: ENDGame: The New Dynamical Core of the Met Office Weather and Climate Prediction Model, in: UK Success Stories in Industrial Mathematics, pp. 27–33, Springer International Publishing, Cham, https://doi.org/10.1007/978-3-319-25454-8_4, 2016.

https://doi.org/10.5194/egusphere-2026-932
Preprint. Discussion started: 10 June 2026

Tørseth, K., Aas, W., Breivik, K., Fjæraa, A. M., Fiebig, M., Hjellbrekke, A. G., Lund Myhre, C., Solberg, S., and Yttri, K. E.: Introduction to the European Monitoring and Evaluation Programme (EMEP) and observed atmospheric composition change during 1972ndash;2009, Atmospheric Chemistry and Physics, 12, 5447–5481, https://doi.org/10.5194/acp-12-5447-2012, 2012.

Tröstl, J., Chuang, W. K., Gordon, H., Heinritzi, M., Yan, C., Molteni, U., Ahlm, L., Frege, C., Bianchi, F., Wagner, R., Simon, M., Lehtipalo, K., Williamson, C., Craven, J. S., Duplissy, J., Adamov, A., Almeida, J., Bernhammer, A. K., Breitenlechner, M., Brilke, S., Dias, A., Ehrhart, S., Flagan, R. C., Franchin, A., Fuchs, C., Guida, R., Gysel, M., Hansel, A., Hoyle, C. R., Jokinen, T., Junninen, H., Kangasluoma, J., Keskinen, H., Kim, J., Krapf, M., Kürten, A., Laaksonen, A., Lawler, M., Leiminger, M., Mathot, S., Möhler, O., Nieminen, T., Onnela, A., Petäjä, T., Piel, F. M., Miettinen, P., Rissanen, M. P., Rondo, L., Sarnela, N., Schobesberger, S., Sengupta, K., Sipilä, M., Smith, J. N., Steiner, G., Tomè, A., Virtanen, A., Wagner, A. C., Weingartner, E., Wimmer, D., Winkler, P. M., Ye, P., Carslaw, K. S., Curtius, J., Dommen, J., Kirkby, J., Kulmala, M., Riipinen, I., Worsnop, D. R., Donahue, N. M., and Baltensperger, U.: The role of low-volatility organic compounds in initial particle growth in the atmosphere, Nature, 533, 527–531, https://doi.org/10.1038/nature18271, 2016.

Usoskin, I. G., Kovaltsov, G. A., and Mironova, I. A.: Cosmic ray induced ionization model CRAC:CRII: An extension to the upper atmosphere, Journal of Geophysical Research: Atmospheres, 115, https://doi.org/https://doi.org/10.1029/2009JD013142, 2010.

Valerino, M. J., Johnson, J. J., Izumi, J., Orozco, D., Hoff, R. M., Delgado, R., and Hennigan, C. J.: Sources and composition of PM2.5 in the Colorado Front Range during the DISCOVER-AQ study, Journal of Geophysical Research: Atmospheres, 122, 566–582, https://doi.org/https://doi.org/10.1002/2016JD025830, 2017.

Vehkamäki, H., Kulmala, M., Napari, I., Lehtinen, K. E. J., Timmreck, C., Noppel, M., and Laaksonen, A.: An improved parameterization for sulfuric acid–water nucleation rates for tropospheric and stratospheric conditions, Journal of Geophysical Research, 107, 4622, https://doi.org/10.1029/2002JD002184, 2002.

Vu, K. T., Dingle, J. H., Bahreini, R., Reddy, P. J., Apel, E. C., Campos, T. L., DiGangi, J. P., Diskin, G. S., Fried, A., Herndon, S. C., Hills, A. J., Hornbrook, R. S., Huey, G., Kaser, L., Montzka, D. D., Nowak, J. B., Pusede, S. E., Richter, D., Roscioli, J. R., Sachse, G. W., Shertz, S., Stell, M., Tanner, D., Tyndall, G. S., Walega, J., Weibring, P., Weinheimer, A. J., Pfister, G., and Flocke, F.: Impacts of the Denver Cyclone on regional air quality and aerosol formation in the Colorado Front Range during FRAPPÉ 2014, Atmospheric Chemistry and Physics, 16, 12 039–12 058, https://doi.org/10.5194/acp-16-12039-2016, 2016.

Wall, C. J., Norris, J. R., Possner, A., McCoy, D. T., McCoy, I. L., and Lutsko, N. J.: Assessing effective radiative forcing from aerosol–cloud interactions over the global ocean, Proceedings of the National Academy of Sciences, 119, e2210481 119, https://doi.org/10.1073/pnas.2210481119, 2022.

Walters, D., Baran, A. J., Boutle, I., Brooks, M., Earnshaw, P., Edwards, J., Furtado, K., Hill, P., Lock, A., Manners, J., Morcrette, C., Mulcahy, J., Sanchez, C., Smith, C., Stratton, R., Tennant, W., Tomassini, L., Van Weverberg, K., Vosper, S., Willett, M., Browse, J., Bushell, A., Carslaw, K., Dalvi, M., Essery, R., Gedney, N., Hardiman, S., Johnson, B., Johnson, C., Jones, A., Jones, C., Mann, G., Milton, S., Rumbold, H., Sellar, A., Ujiie, M., Whitall, M., Williams, K., and Zerroukat, M.: The Met Office Unified Model Global Atmosphere 7.0/7.1 and JULES Global Land 7.0 configurations, Geoscientific Model Development, 12, 1909–1963, https://doi.org/10.5194/gmd-12-1909-2019, 2019.

Wang, M. and Penner, J. E.: Aerosol indirect forcing in a global model with particle nucleation, Atmospheric Chemistry and Physics, 9, 239–260, https://doi.org/10.5194/acp-9-239-2009, 2009.

Wang, M., Xiao, M., Bertozzi, B., Marie, G., Rörup, B., Schulze, B., Bardakov, R., He, X.-C., Shen, J., Scholz, W., Marten, R., Dada, L., Baalbaki, R., Lopez, B., Lamkaddam, H., Manninen, H. E., Amorim, A., Ataei, F., Bogert, P., Brasseur, Z., Caudillo, L., De Menezes, L.-P., Duplissy, J., Ekman, A. M. L., Finkenzeller, H., Carracedo, L. G., Granzin, M., Guida, R., Heinritzi, M., Hofbauer, V., Höhler,

https://doi.org/10.5194/egusphere-2026-932
Preprint. Discussion started: 10 June 2026

K., Korhonen, K., Krechmer, J. E., Kürten, A., Lehtipalo, K., Mahfouz, N. G. A., Makhmutov, V., Massabò, D., Mathot, S., Mauldin, R. L., Mentler, B., Müller, T., Onnela, A., Petäjä, T., Philippov, M., Piedehierro, A. A., Pozzer, A., Ranjithkumar, A., Schervish, M., Schobesberger, S., Simon, M., Stozhkov, Y., Tomé, A., Umo, N. S., Vogel, F., Wagner, R., Wang, D. S., Weber, S. K., Welti, A., Wu, Y., Zauner-Wieczorek, M., Sipilä, M., Winkler, P. M., Hansel, A., Baltensperger, U., Kulmala, M., Flagan, R. C., Curtius, J., Riipinen, I., Gordon, H., Lelieveld, J., El-Haddad, I., Volkamer, R., Worsnop, D. R., Christoudias, T., Kirkby, J., Möhler, O., and Donahue, N. M.: Synergistic HNO3–H2SO4–NH3 upper tropospheric particle formation, Nature, 605, 483–489, 2022.

Wang, X., Gordon, H., Grosvenor, D. P., Andreae, M. O., and Carslaw, K. S.: Contribution of regional aerosol nucleation to low-level CCN in an Amazonian deep convective environment: results from a regionally nested global model, Atmospheric Chemistry and Physics, 23, 4431–4461, https://doi.org/10.5194/acp-23-4431-2023, 2023.

Weber, R. J., Marti, J. J., McMurry, P. H., Eisele, F. L., Tanner, D. J., and Jefferson, A.: Measured atmospheric new particle formation rates: Implications for nucleation mechanisms, Chemical Engineering Communications, 151, 53–64, https://doi.org/10.1080/00986449608936541, 1996.

Westervelt, D. M., Pierce, J. R., Riipinen, I., Trivitayanurak, W., Hamed, A., Kulmala, M., Laaksonen, A., Decesari, S., and Adams, P. J.: Formation and growth of nucleated particles into cloud condensation nuclei: model–measurement comparison, Atmospheric Chemistry and Physics, 13, 7645–7663, https://doi.org/10.5194/acp-13-7645-2013, 2013.

Williamson, C. J., Kupc, A., Axisa, D., Bilsback, K. R., Bui, T. P., Campuzano-Jost, P., Dollner, M., Froyd, K. D., Hodshire, A. L., Jimenez, J. L., Kodros, J. K., Luo, G., Murphy, D. M., Nault, B. A., Ray, E. A., Weinzierl, B., Wilson, J. C., Yu, F., Yu, P., Pierce, J. R., and Brock, C. A.: A large source of cloud condensation nuclei from new particle formation in the tropics, https://doi.org/10.1038/s41586-019-1638-9, 2019.

Wilson, D. R. and Ballard, S. P.: A microphysically based precipitation scheme for the UK meteorological office unified model, Quarterly Journal of the Royal Meteorological Society, 125, 1607–1636, https://doi.org/10.1002/qj.49712555707, 1999.

Wilson, D. R., Bushell, A. C., Kerr-Munslow, A. M., Price, J. D., and Morcrette, C. J.: PC2: A prognostic cloud fraction and condensation scheme. I: Scheme description, Quarterly Journal of the Royal Meteorological Society, 134, 2093–2107, https://doi.org/10.1002/qj.333, 2008.

Wohl, C., Villamayor, J., Galí, M., Mahajan, A. S., Fernández, R. P., Cuevas, C. A., Bossolasco, A., Li, Q., Kettle, A. J., Williams, T., Sarda-Esteve, R., Gros, V., Simó, R., and Saiz-Lopez, A.: Marine emissions of methanethiol increase aerosol cooling in the Southern Ocean, Science Advances, 10, eadq2465, https://doi.org/10.1126/sciadv.adq2465, 2024.

Wood, N., Staniforth, A., White, A., Allen, T., Diamantakis, M., Gross, M., Melvin, T., Smith, C., Vosper, S., Zerroukat, M., and Thuburn, J.: An inherently mass-conserving semi-implicit semi-Lagrangian discretization of the deep-atmosphere global non-hydrostatic equations, Quarterly Journal of the Royal Meteorological Society, 140, 1505–1520, https://doi.org/10.1002/qj.2235, 2014.

Woodward, S.: Modeling the atmospheric life cycle and radiative impact of mineral dust in the Hadley Centre climate model, Journal of Geophysical Research: Atmospheres, 106, 18 155–18 166, https://doi.org/10.1029/2000JD900795, 2001.

Yan, C., Yin, R., Lu, Y., Dada, L., Yang, D., Fu, Y., Kontkanen, J., Deng, C., Garmash, O., Ruan, J., Baalbaki, R., Schervish, M., Cai, R., Bloss, M., Chan, T., Chen, T., Chen, Q., Chen, X., Chen, Y., Chu, B., DÃllenbach, K., Foreback, B., He, X., Heikkinen, L., Jokinen, T., Junninen, H., Kangasluoma, J., Kokkonen, T., Kurppa, M., Lehtipalo, K., Li, H., Li, H., Li, X., Liu, Y., Ma, Q., Paasonen, P., Rantala, P., Pileci, R. E., Rusanen, A., Sarnela, N., Simonen, P., Wang, S., Wang, W., Wang, Y., Xue, M., Yang, G., Yao, L., Zhou, Y., Kujansuu, J., Petaja, T., Nie, W., Ma, Y., Ge, M., He, H., Donahue, N. M., Worsnop, D. R., Kerminen, V.-M., Wang, L., Liu, Y., Zheng, J., Kulmala, M., Jiang, J., and Bianchi, F.: The Synergistic Role of Sulfuric Acid, Bases, and Oxidized Organics Governing New-Particle Formation

https://doi.org/10.5194/egusphere-2026-932
Preprint. Discussion started: 10 June 2026

in Beijing, Geophysical Research Letters, 48, e2020GL091 944, https://doi.org/https://doi.org/10.1029/2020GL091944, e2020GL091944 2020GL091944, 2021.

Yu, F. and Luo, G.: Simulation of particle size distribution with a global aerosol model: contribution of nucleation to aerosol and CCN number concentrations, Atmospheric Chemistry and Physics, 9, 7691–7710, https://doi.org/10.5194/acp-9-7691-2009, 2009.

Yu, F., Nadykto, A. B., Herb, J., Luo, G., Nazarenko, K. M., and Uvarova, L. A.: H₂SO₄-H₂O-NH₃ ternary ion-mediated nucleation (TIMN): Kinetic-based model and comparison with CLOUD measurements, Atmospheric Chemistry and Physics Discussions, pp. 1–41, https://doi.org/10.5194/acp-2018-396, 2018.

Yu, F., Nadykto, A. B., Luo, G., and Herb, J.: H_2SO_4–H_2O binary and H_2SO_4–H_2O–NH_3 ternary homogeneous and ion-mediated nucleation: lookup tables version 1.0 for 3-D modeling application, Geoscientific Model Development, 13, 2663–2670, https://doi.org/10.5194/gmd-13-2663-2020, 2020.

Zhang, K., Feichter, J., Kazil, J., Wan, H., Zhuo, W., Griffiths, A. D., Sartorius, H., Zahorowski, W., Ramonet, M., Schmidt, M., Yver, C., Neubert, R. E. M., and Brunke, E.-G.: Radon activity in the lower troposphere and its impact on ionization rate: a global estimate using different radon emissions, Atmospheric Chemistry and Physics, 11, 7817–7838, https://doi.org/10.5194/acp-11-7817-2011, 2011.

Zhang, R., Suh, I., Zhao, J., Zhang, D., Fortner, E. C., Tie, X., Molina, L. T., and Molina, M. J.: Atmospheric New Particle Formation Enhanced by Organic Acids, Science, 304, 1487–1490, https://doi.org/10.1126/science.1095139, 2004.

Zhao, B., Shrivastava, M., Donahue, N. M., Gordon, H., Schervish, M., Shilling, J. E., Zaveri, R. A., Wang, J., Andreae, M. O., Zhao, C., Gaudet, B., Liu, Y., Fan, J., and Fast, J. D.: High concentration of ultrafine particles in the Amazon free troposphere produced by organic new particle formation, Proceedings of the National Academy of Sciences, 117, 25 344–25 351, https://doi.org/10.1073/pnas.2006716117, 2020.

Zhao, B., Donahue, N. M., Zhang, K., Mao, L., Shrivastava, M., Ma, P.-L., Shen, J., Wang, S., Sun, J., Gordon, H., et al.: Global variability in atmospheric new particle formation mechanisms, Nature, 631, 98–105, 2024.